

**The genomic landscape, causes, and consequences of extensive phylogenomic discordance
in murine rodents**

Gregg W. C. Thomas^{1,2,*}, Jonathan J. Hughes^{3,4}, Tomohiro Kumon⁵, Jacob S. Berv^{3,6}, C. Erik Nordgren⁵, Michael Lampson⁵, Mia Levine⁵, Jeremy B. Searle³, Jeffrey M. Good¹

¹*Division of Biological Sciences, University of Montana, Missoula, MT, 59801.*

²*Informatics Group, Harvard University, Cambridge, MA, 02138*

³*Department of Ecology and Evolutionary Biology, Cornell University, Ithaca, NY, 14853.*

⁴*Department of Evolution, Ecology, and Organismal Biology, University of California Riverside, Riverside, CA, 92521*

⁵*Department of Biology, University of Pennsylvania, Philadelphia, PA, 19104*

⁶*Department of Ecology and Evolutionary Biology, University of Michigan, Ann Arbor, MI, 48109*

*Corresponding author

E-mail: gthomas@fas.harvard.edu

Abstract

A species tree is a central concept in evolutionary biology whereby a single branching phylogeny reflects relationships among species. However, the phylogenies of different genomic regions often differ from the species tree. Although tree discordance is widespread in phylogenomic studies, we still lack a clear understanding of how variation in phylogenetic patterns is shaped by genome biology or the extent to which discordance may compromise comparative studies. We characterized patterns of phylogenomic discordance across the murine rodents – a large and ecologically diverse group that gave rise to the laboratory mouse and rat model systems. Combining recently published linked-read genome assemblies for seven murine species with other available rodent genomes, we first used ultra-conserved elements (UCEs) to infer a robust time-calibrated species tree. We then used whole genomes to examine finer-scale patterns of discordance across ~12 million years of divergence. We found that proximate chromosomal regions tended to have more similar phylogenetic histories. There was no clear relationship between local tree similarity and recombination rates in house mice, but we did observe a correlation between recombination rates and average similarity to the species tree. We also detected a strong influence of linked selection whereby purifying selection at UCEs led to appreciably less discordance. Finally, we show that assuming a single species tree can result in substantial deviation from the results with gene trees when testing for positive selection under different models. Collectively, our results highlight the complex relationship between phylogenetic inference and genome biology and underscore how failure to account for this complexity can mislead comparative genomic studies.

Keywords: *phylogenetic discordance, murine rodents, molecular evolution recombination, genomics, mouse*

Significance Statement

Genomic data has demonstrated that when sequences from multiple species are compared, different regions of the genome exhibit different phylogenetic histories. These discordant histories could be due to either biological processes, such as ancestral variation or introgression, or artifacts of the inference process. We use the genomes of several murine rodents to distinguish how features of the genome, such as recombination rates, genes, and other conserved regions, affect this discordance across the genome. Considering the prevalence of discordance across the genome, we also test how using a single species tree, a common practice, affects inferences from tests for positive selection. Our study shows that conserved genomic loci exhibit lower amounts of discordance, and that discordance can negatively affect inferences of selection.

Introduction

Phylogenies are the unifying concept in understanding the evolution of species, traits, and genes. However, extensive high-throughput sequencing data has now revealed that evolutionary relationships between species are often not well represented by a single phylogeny (Edwards 2009; Hahn and Nakhleh 2016). While a dominant signal of bifurcating speciation usually exists (*i.e.*, a species tree), phylogenetic signal that may disagree with species relationships can arise from ancestral polymorphisms (incomplete lineage sorting; ILS), gene flow (introgression), and gene duplication and loss (Maddison 1997). The theoretical prediction of phylogenetic discordance has long been appreciated (Hudson 1983; Pamilo and Nei 1988; Maddison 1997; Rosenberg 2002), but empirical evidence now emphasizes just how extensive discordance can be among a set of species (Feng, et al. 2022; Gable, et al. 2022; Smith, et al. 2023). For example, studies of birds (Jarvis, et al. 2014), mammals (Ferreira, et al. 2021; Lopes, et al. 2021; Foley, et al. 2024), plants (Pease, et al. 2016), and insects (Sun, et al. 2021; He, et al. 2023) have found that with extensive taxon sampling and genomic data, highly supported species tree topologies are rarely or never exactly recovered in the underlying gene trees. Whereas these examples highlight the prevalence of phylogenetic discordance across the tree of life, we still lack a clear understanding of how phylogenetic patterns are shaped by the details of genome biology or the extent to which discordance may compromise inferences from comparative studies that assume a singular species history.

In practice, failure to acknowledge and account for phylogenetic discordance could severely affect biological inference. Analyses of molecular evolution are usually performed on a gene-by-gene basis (Pond, et al. 2005; Yang 2007; Hu, et al. 2019; Kowalczyk, et al. 2019), but it is still common practice to assume a single genome-wide species tree for each locus. For gene-based analyses, using the wrong tree may cause erroneous inferences of positive directional selection, convergent evolution, and genome-wide inferences of correlated rate variation (Mendes, et al. 2016). Phylogenetic discordance can also affect how continuous traits are reconstructed across phylogenies, as the genes that underly these traits may not follow the species history (Avice and Robinson 2008; Hahn and Nakhleh 2016; Mendes, et al. 2018; Hibbins, et al. 2023). In these instances, phylogenetic discordance may need to be characterized and incorporated into the experimental and analytical design. Alternatively, if a researcher's primary questions are focused on reconstructing the evolutionary history of speciation (*i.e.*, the species tree), then phylogenetic discordance may obscure the true signal of speciation (Fontaine, et al. 2015; Foley, et al. 2024). In this case, knowledge about patterns of discordance across genomes could inform decisions about locus selection, data filtering, and model parameters during species tree reconstruction.

Given these considerations, a better understanding of the genomic context of phylogenetic discordance is warranted. Although often conceptualized primarily as a stochastic consequence of population history (Maddison 1997), patterns of phylogenetic discordance are likely to be non-random and dependent on localized patterns of genetic drift, natural selection, recombination, and mutation (Johri, et al. 2022). Discordance due to ILS ultimately depends on effective population sizes across the branches of the phylogeny (Pamilo and Nei 1988; Degnan and Rosenberg 2006)

and, therefore, should covary with any process that influences local patterns of genetic diversity (e.g., linked negative or positive selection). Likewise, discordance due to introgression may be influenced by selection against incompatible alleles or positive selection for beneficial variants (Lewontin and Birch 1966; Jones, et al. 2018). Selection, ILS, and introgression, are expected to leave different genomic signals that should allow us to test hypotheses about both the cause and the scale of phylogenetic discordance (Huson, et al. 2005; Kulathinal, et al. 2009; Green, et al. 2010; Vanderpool, et al. 2020). Yet the genomic context of phylogenetic discordance has remained elusive. For example, localized patterns of phylogenetic discordance should be influenced by patterns of recombination (Hudson and Kaplan 1988) and simulation studies confirm that the closer two regions are in the genome, the more history they share (Slatkin and Pollack 2006; McKenzie and Eaton 2020). However, empirical studies have been inconclusive regarding the relationship between discordance and recombination rates, ranging from no relationship in great apes (Hobolth, et al. 2007), a weak positive correlation in house mice (White, et al. 2009), a strong positive correlation broadly across primates (Rivas-Gonzalez, et al. (2023), or increased discordance in regions of lower recombination (Scally, et al. 2012; Pease and Hahn 2013). Thus, it remains unclear how phylogenetic discordance scales locally across the genome as a function of recombination and the strength of linked selection, pointing to the need for empirical studies in systems with sufficient genomic resources to explore the causes of discordance.

To investigate the causes and consequences of phylogenetic discordance, we took advantage of genomic resources available for house mice (*Mus musculus*). This rodent species is one of the most important mammalian model systems for biological and biomedical research and is embedded within a massive radiation of rats and mice (Murinae). This ecologically diverse and species-rich group is comprised of over 600 species and makes up >10% of all mammalian species, and yet is only about 15 million years old, making this system an excellent choice for phylogenetic studies over both short and long timescales. Despite the power of evolution-guided functional and biomedical analysis (Christmas, et al. 2023), relatively few murine genomes have been sequenced outside of *Mus* and *Rattus*.

We analyze recently sequenced genomes for seven murine species (*Mastomys natalensis*, *Hylomyscus alleni*, *Praomys delectorum*, *Rhabdomys dilectus*, *Grammomys dolichurus*, *Otomomys typus*, and *Rhynchomys soricoides*) sampled from across this radiation (Kumon, et al. 2021). We combine these new genomes with previously sequenced genomes and genomic resources from the *M. musculus* model system to study phylogenetic relationships within Murinae as well as the landscape of discordance along rodent chromosomes. We first inferred a species tree for these and other sequenced rodent genomes, focusing on signals derived from commonly used ultra-conserved elements (UCEs). We used these UCE data to infer a robust, time-calibrated phylogeny of sequenced murine rodents, providing a useful resource for future comparative studies within this important group. Using this species tree, we then used a subset of whole genomes to study how phylogenetic discordance is related to species-level inferences of relatedness, recombination rate, and patterns of molecular evolution. Using genetic maps and functional annotation from the powerful house mouse system, we test several hypotheses linking spatial patterns of discordance

to genetic drift, natural selection, and recombination. Finally, we show how the use of a single species-tree impacts gene-level inferences from common molecular evolution tests for natural selection in these species. Collectively, our results advance our understanding of how core features of genome biology influence underlying phylogenetic patterns, the extent to which established model system resources can be leveraged for broader phylogenetic studies, and the consequences of ignoring phylogenetic uncertainty.

Results

Estimation of a murine species tree

Using a concatenated dataset of 2,632 aligned ultra conserved elements (UCEs), we inferred a species tree of 18 murine rodent species (Figure 1; Table S1) that recovered the same relationships as previous reconstructions of Murinae using a small number of loci (Lecompte, et al. 2008; Steppan and Schenk 2017). The species tree inferred from a quartet-based summary of the gene tree topologies was identical to the concatenated tree (Figure S1). While bootstrap and SH-aLRT values provided high support to our inferred species trees (Figure 1), we found evidence for considerable discordance across individual UCE phylogenies. The five shortest branches in the concatenated tree had a site concordance factor (sCF) of less than 50%, suggesting that alternate resolutions of the quartet had equivocal support (Figure S2). Gene concordance factors (gCF) for each branch in the species tree were on aggregate much higher, with all but four branches supported by almost every gene tree in the analysis and with the lowest values likely being driven by a several short internal branches (Figure S2). This pattern was recapitulated using a quartet-based summary method (Figs. S1 and S3). At the two most discordant nodes (E and J in Figure 1), the recovered topology was supported by approximately one third of all gene trees.

We estimated divergence times for the inferred concatenated phylogeny (Figure 1; Table S2) using four fossil calibration points (Table S3). The murid and cricetid groups had an estimated divergence time of 22.66 Ma (node A in Figure 1) followed by the Murinae and the Gerbillinae at 21.34 Ma (B), albeit with wide confidence intervals (CI) in both cases. The core Murinae (C) *sensu* Steppan et al. (2005) are inferred to have arisen 13.11 Ma (CI: 11.42 – 15.10). Hydromyini then split off at 12.15 Ma (D, CI: 11.10 – 13.51) followed by Otomyini and Arvicanthini at 11.70 Ma (E, fossil calibration from Kimura, et al 2015). The remaining Murine tribes evolved in rapid succession, with Apodemini diverging from Murini and Praomyini at 10.84 Ma (F). Murini and Praomyini then split at 10.19 Ma (H). The two *Rattus* species in our dataset were inferred to have diverged 2.01 Ma (Q, CI: 1.26 – 2.30). This dated UCE phylogeny is congruent with previous works (Lecompte, et al. 2008; Steppan and Schenk 2017) and provides context on the evolutionary timescale upon which we next describe the genomic landscape of phylogenetic discordance across a collection of murine genomes.

The landscape of phylogenetic discordance along murine genomes

We analyzed genome-wide phylogenetic histories of six recently sequenced murine rodent genomes and the *M. musculus* reference genome spanning approximately 12 million years of divergence (see Figure 1). Using the *M. musculus* coordinate system, we partitioned and aligned 263,389 non-overlapping 10 kb windows from these seven species (Table S1). After filtering windows in repetitive regions or with low phylogenetic signal, we recovered 163,765 trees with an average of 616 informative sites per window (Figure S4).

Phylogenetic discordance was pervasive within and between chromosomes. We inferred 597 of the 945 possible unique rooted topologies among six species (when specifying *R. soricoides* as the outgroup) across all chromosomes. The number of unique topologies per chromosome ranged from 75 to 218 (mean = 141). However, just four different topologies were ranked in the top three per chromosome. (Fig 2A; File S1) and only nine trees were present at a frequency above 1%. Among these, the top three topologies only differed in the ordering of the clade containing *Hylomyscus alleni*, *Mastomys natalensis*, and *Praomys delectorum* (HMP clade). This clade also showed the second lowest concordance in the species tree inferred from UCEs (Figure 1, node J). These three topologies comprise between 13-15% of all recovered topologies (Figure 2). Interestingly, the least common of these three trees (13.1%) matched the topology recovered via concatenation of all coding regions and the species tree recovered from UCEs (Figure 1). That is, the robustly inferred species tree did not match the evolutionary relationships inferred for over 85% of the genome.

While visual inspection revealed no clear partitioning of topological structures along chromosomes (e.g., Figure 2C), we found that phylogenies were not randomly distributed across mouse chromosomes. Using the weighted Robinson-Foulds metric, we found that tree similarity between windows decayed logarithmically along chromosomes (Figure 3A and B), and the distance at which tree similarity appeared random varied considerably among chromosomes ranging from 0.15 Megabases (Mb) on chromosome 17 to 141.29 Mb on the chromosome 2 (Figure 3C, Figure S5). While chromosomes 2, 7, 9, and 11 were autosomal outliers with distances between windows to random-like trees exceeding 25 Mb, the average distance among all other autosomes was only 2.1 Mb. The rates at which phylogenetic similarity decayed tended to be inversely proportional to the distance at which two randomly drawn phylogenies lost similarity (Figure 3D).

Next, we performed a pairwise alignment of the reference mouse and rat genomes to assess how large structural variations, such as inversions and translocations, may influence our inferences of phylogenetic relatedness along the genome. These species span the deepest divergence of the sample for which we assessed genome-wide discordance, so the level of large structural variation present among them should give us an idea of the amount of ancestral variation in our sample. The mouse and rat genomes were mostly co-linear for large, aligned chunks, with large translocations and inversions on mouse chromosomes 5, 8, 10, 13, and 16 (Figure S6). We also observe large-scale inversions on chromosome 16. We found that, while most chromosomes were co-linear between mouse and rat, the average size of the 307,275 contiguously aligned chunks averages under 10 kb, with the average distance between aligned segments being between 2,380 bp on the mouse genome and 4,927 bp on the rat chromosome (Figure S7). This pattern presents two major

implications for our analyses. First, we could not transpose the coordinate system from mouse to rat with enough resolution to use genetic maps from rat. Second, most other structural variations in our sample appear likely to be small insertions of transposable elements (e.g., SINEs ~150-500 bp, LINEs ~4-7kb; Platt, et al. 2018) that should have a negligible effect on discordance analyses since our window size is much larger and we excluded windows that were made up of mostly repeats.

Discordance with recombination rate and other genomic features

Using markers from genetic crosses within *M. musculus* (Shifman, et al. 2006; Cox, et al. 2009) we examined whether regions with high recombination also showed more phylogenetic discordance over short genetic distances when compared to regions with low recombination. Specifically, we calculated recombination rates within 5 Mb windows (Figure S8) and then measured tree similarity between the first and last 10 kb window ($R^2 = 3.0e-9$; $p = 0.99$; Figure 4A) and the rate at which tree similarity changes between the first 10 kb window and every other 10 kb window ($R^2 = 0.003$; $p = 0.11$; Figure 4B). Surprisingly, we found no relationship between tree similarity and recombination rates measured at this scale. However, we did observe a slight positive correlation between recombination rate and dissimilarity to the species tree when averaging wRF over all 10 kb window trees within a 5 Mb recombination window ($R^2 = 0.05$; $p = 7.6e-8$; Figure 4C). We also examined regions of the genome centered on recombination hotspots identified in *M. musculus* (Smagulova, et al. 2011) and found that these regions had significantly slower rates of decay in similarity over genomic distance compared to windows that were not centered on hotspots ($p = 0.019$; Figure 5A), and that they were also significantly more phylogenetically similar over short distances ($p = 0.015$; Figure 5B). Thus, when taken as a whole, we found that regions of higher recombination rates in house mice did not show more local phylogenetic discordance *per se* but did tend to show more discordance relative to the genome-wide species tree.

Evolutionary relationships around certain conserved genomic features may also be shaped by locally reduced effective population sizes due to a history of pervasive linked negative or positive selection. To test for this, we measured tree similarity in 10 kb windows around all annotated protein-coding genes, ultra-conserved elements (UCEs), and protein-coding genes identified as evolving rapidly (*i.e.*, significantly elevated d_N/d_S) due to positive directional selection and compared these patterns relative to chromosome-wide trends (*i.e.*, windows without annotated features). In general, UCEs showed more local phylogenetic similarity among adjacent windows (*i.e.*, less discordance) than regions surrounding recombination hotspots ($p = 2.42e-12$), coding genes ($p = 4.65e-14$), rapidly evolving coding genes ($p = 1.56e-6$), and windows that did not include any of these features ($p = 5.02e-14$; Figure 5A). In contrast, protein-coding genes (including rapidly evolving genes) were indistinguishable from background rates of discordance observed in windows without annotated genomic features (Figure 5A). Likewise, UCEs were also much more similar to the overall species tree when compared to any other feature (Figure 5B). Unlike our test of local discordance, protein-coding genes also showed less species tree

discordance than windows containing no features or recombination hotspots, but the effect was much less pronounced than observed at UCEs.

Consequences of tree specification on analyses of molecular evolution

Next, we examined how phylogenetic discordance influenced inferences on the evolution of protein-coding sequences. Among a set of 22,261 *M. musculus* protein-coding transcripts, the average distance between the start and end of the coding sequence was 37.02 kb, or roughly 4 non-overlapping 10 kb windows. At this distance, tree similarity is predicted to diminish considerably (e.g., by 0.10 wRF units), such that the phylogenetic history of individual genes may often contain some phylogenetic discordance (Mendes and Hahn 2016; Mendes, et al. 2019). We also found that out of the 67,566 times the coding sequence in a gene overlapped with a 10 kb window, the inferred topology of the gene tree exactly matched the topology of the corresponding window tree only 11% of the time. Thus, the common practice of inferring gene trees on concatenated coding exons from a single transcript is still likely averaging over multiple possible albeit correlated histories.

Finally, we tested how tree misspecification might impact standard d_N/d_S based phylogenetic analyses for positive directional selection. Specifically, we used the still common practice of assuming a single species tree for all genes and compared that to using individually inferred gene trees in three common statistical tests for positive selection: PAML's M1a vs. M2a test (Yang 2007), HyPhy's BUSTED test (Murrell, et al. 2015), and HyPhy's aBSREL test (Smith, et al. 2015a). We found that many genes were inferred as having experienced positive directional selection when using a single species tree, but not when using gene trees and vice versa (Figure 6). The extent to which the single species tree differed from the gene trees for the different types of selection test is documented in Table 1. For BUSTED, we observe that 28% of genes inferred as having evolved under positive directional selection when using the gene tree were not inferred when using the concatenated species tree. The opposite was true for M1a vs. M2a, where, among genes showing inconsistent evidence for positive selection across the two scenarios, 76% do so when using the concatenated species tree but not individual gene trees. In general, genes found to be evolving under positive selection using both tree types tended to be more concordant with the species tree than those that had evidence for positive selection either using only the concatenated tree or the gene tree (Figure 6).

Discussion

Phylogenies provide insight into the relationships of species and serve as a framework for asking questions about molecular and trait evolution. However, phylogenetic histories vary extensively across regions of a genome as a simple consequence of population genetic processes, and evolutionary relationships between species may not often be well represented by a single representative species-level phylogeny. Here, we combine the resources of the house mouse (*Mus musculus*) with new and recently published (Kumon et al. 2021) genomes from seven species to understand the systematics of murine rodents and causes and consequences of phylogenetic

discordance along murine genomes. These new analyses help to place this important model system in a stronger evolutionary context and begin to fill the gap in genome sampling of murine rodents, which, despite their exceptional morphological and ecological diversity and species richness, have had relatively few whole genomes sequenced. We use these genomic resources to study the landscape of phylogenetic discordance across the genome, understand how recombination and natural selection shape phylogenetic histories, and evaluate how assuming a single evolutionary history can compromise the study of molecular evolution in an important biomedical model system.

Phylogenomic relationships of murine rodent lineages from conserved genomic regions

The extraordinary species richness of murine rodents complicates phylogenetic analyses because of the resources required to sample, sequence, and analyze such widely distributed taxa. Earlier work either attempted to resolve specific groups such as *Mus* (Lundrigan, et al. 2002; Suzuki, et al. 2004) and *Apodemus* (Serizawa, et al. 2000; Liu, et al. 2004), or to uncover broader relationships across the subfamily (Martin, et al. 2000; Steppan, et al. 2005) based on a few genetic markers. Lecompte et al. (2008) provided one of the earliest well-supported phylogenetic reconstructions from across Murinae and the tribal classifications they proposed remain generally supported. More recent work has increased the number of taxa sampled, both for analyses of Murinae specifically (Pagès, et al. 2016) and for their placement within Muridae and Muroidea (Schenk, et al. 2013; Steppan and Schenk 2017; Rowe, et al. 2019) albeit based on a limited number of loci. More recent studies have greatly expanded the number of loci used for phylogenetic inference (Mikula, et al. 2021), including the use of 1,245 exons (Roycroft, et al. 2020) and 1,360 exons (Roycroft, et al. 2021), but have focused on specific tribes within Murinae.

Our inferred species tree based on 2,632 UCEs from 18 species across the radiation (Figure 1) is consistent with previous studies (Lecompte, et al. 2008; Steppan and Schenk 2017; Aghova, et al. 2018). Branch support was uniformly high, and gene trees unambiguously support the tribal classification of Lecompte, et al. (2008). However, four shorter branches show more substantial gene tree discordance (Figure 1, branches D, E, H, and J), with two recovered clades (E and J) being supported by less than half of all gene trees. We also estimated divergence times on our inferred species tree using four fossil calibration points (Table S3), recovering times that are roughly consistent with the relatively young estimates found by (Steppan and Schenk 2017) (see Supplement). This dated species tree provides an evolutionary timescale to evaluate the genomic landscape of phylogenetic discordance across ~12 my of murine evolution.

The genomic landscape of phylogenetic discordance

Limiting the number and nature of the loci used to resolve species relationships is often useful to get an initial picture of the history of speciation across many taxa. However, such targeted approaches may fail to capture the degree of discordance driven by incomplete lineage sorting and introgression (Alexander, et al. 2017; Chan, et al. 2020; Vanderpool, et al. 2020; Alda, et al. 2021).

Our results highlight the limitations of reduced marker-based approaches and the general relationships between phylogenetic patterns and functional attributes of the genome in several interesting ways. Using the house mouse genome annotation, we found that the species tree inferred from only genes or UCEs did not match evolutionary relationships inferred for over 85% of the genome. Although similar frequencies were observed among these three most common trees (Figure 2), the topology robustly inferred from genes or UCEs was not that common overall and only the third most frequent topology among 10 kb windows genome-wide. This result was driven mainly by discordance among three more closely related (*Praomyini*) species sampled for this study, which had nodes with low concordance in the UCE species tree (Fig 1, node J). In the window analysis, each alternate topology of this clade occurred at a frequency of ~14% while the rest of the topology remained consistent with the species tree (Figure 2), indicating that the alternate topologies are caused by high levels of ILS at these nodes. Increased discordance at unresolved nodes is a common feature of phylogenomic datasets. These patterns illustrate how extensive discordance can arise even in a small sample of species and underscores that a single inferred species tree often may not capture the history of individual regions of the genome.

Given the fundamental role that recombination should play in shaping patterns of genetic variation within genomes, it is reasonable to assume that patterns of ILS should be broadly shaped by local recombination rate. We did not observe a clear relationship between local recombination rates in mice (*M. musculus*) and the degree of local phylogenetic discordance (i.e., phylogenetic similarity over 5 Mb intervals). However, we did find that regions of high recombination rate tended to be more discordant with the inferred species tree, in line with findings in mammals (Pease and Hahn 2013; Foley, et al. 2023; Rivas-Gonzalez, et al. 2023) and *Drosophila* (Pease and Hahn 2013). Recombination rates evolve fairly rapidly both within (Kong, et al. 2002; Cox, et al. 2009; Stapley, et al. 2017) and between mammalian species (Jensen-Seaman, et al. 2004; Ptak, et al. 2005; Stevison, et al. 2016; Stapley, et al. 2017) likely due, in part, to the high turnover of hotspots due to the changing landscape of binding sites for PRDM9 (Baudat, et al. 2010; Singhal, et al. 2015). Similar to findings in great apes (Hobolth, et al. 2007), our results suggest that high-resolution genetic maps from a single species provide some weak predictive value for understanding broader patterns of species tree discordance. However, these limited estimates may not be predictive of finer-scale patterns in a sample spanning over 12 million years of mammalian evolution (but see Foley, et al. 2023). Overall, the evolution of recombination landscapes across closely related species remains an important empirical question in evolutionary genetics (Dapper and Payseur 2017), especially as the generation of chromosome-scale genome assemblies continues to greatly outpace estimates of patterns of recombination within those genomes.

One source of evolution in the recombination map may be changes in synteny. Our reference-guided analyses assume collinearity between *Mus* and the other lineages we are comparing (i.e., no karyotype variation), at least at the window-based scale we are comparing variation. Structural variation, including substantial variation in chromosome numbers, is likely to be widespread in rodents (Stanyon, et al. 1999; Yalcin, et al. 2011; Romanenko, et al. 2012; Keane, et al. 2014) and has the potential to skew our results when comparing tree similarity between

regions of the genome using multiple species. Generating chromosome-scale assemblies may prove limiting for some non-*Mus* and *Rattus* species given that tissue resources for this group are derived from natural history collections that often lack high molecular weight DNA. Nonetheless, whole genome alignments between mouse and rat indicate high degrees of chromosomal synteny and co-linearity (Fig S6), suggesting that many regions will be colinear in our sample.

Natural selection reduces the effective population size (N_e) of genomic regions through genetic hitchhiking of variation linked to the fixation of positively selected mutations (i.e., selective sweeps; Maynard Smith and Haigh 1974; Kaplan, et al. 1989) and the purging of deleterious mutations (i.e., background selection; Charlesworth, et al. 1993; Hudson and Kaplan 1995). Thus, variation in parameters dependent on N_e – such as standing levels of nucleotide variation and patterns of incomplete lineage sorting – should be reduced by linkage to functional elements subject to selection (Johri, et al. 2022). Consistent with this, we observed the lowest rates of local discordance (Figure 5A) and overall gene tree/species tree discordance (Figure 5B) near UCEs when compared to all other genomic features we studied. These results suggest that a history of recurrent purifying selection on UCEs (Katzman, et al. 2007) strongly reduces patterns of discordance through a persistent local reduction in N_e . In contrast, protein coding genes showed rates of local discordance that were similar to background levels, even when considering genes rapidly evolving due to positive directional selection (Figure 5A). However, both classes of genes did show less species tree discordance than background consistent with previous results (Scally, et al. 2012; Rivas-Gonzalez, et al. 2023), but this effect was much weaker than as observed at UCEs (Figure 5B). Collectively, these data suggest that the frequency and strength of selection plays an important role in structuring patterns of incomplete lineage sorting across the genome over deeper evolutionary timescales.

One practical consequence of this is that phylogenetic inferences based on UCE markers would seem less prone to discordance and may provide cleaner estimates of species tree history than randomly chosen or protein-coding regions. Indeed, windows centered on UCEs have a higher degree of similarity to the species tree than other genomic features (i.e., 17% concordance with the species tree, versus 13% genome-wide or 15% for protein-coding genes). However, it is worth noting that UCEs are also more likely to provide a potentially misleading underestimate of genome-wide levels of discordance. Given this relationship, species tree inferences based on UCEs should likely not, for example, be extended to related population genetic parameters of interest (e.g., ancestral population sizes, estimates population genetic diversity), and could mislead the reconstruction of protein (see below) or trait evolution across phylogenies (Avisé and Robinson 2008; Hahn and Nakhleh 2016; Mendes, et al. 2018; Hibbins, et al. 2023). Finally, despite the relative ease of generating UCE data, such markers are likely unsuitable for genetic inferences within populations given the pervasive effects of linked selection.

Discordance and Molecular Evolution

We also found that the choice of tree topology significantly affects the results from various common tests for positive selection. Previous studies have used simulations to show that tree

misspecification can lead to incorrect placement of substitutions on branches, possibly leading to spurious results for tests of positive directional selection within empirical datasets (Mendes and Hahn 2016). Here, we use empirical data in mice to document the extent that using local gene trees versus assuming an overall species tree may shape inferences of positive directional selection on protein-coding sequences.

For each of the three selection tests run (*i.e.*, HyPhy's BUSTED and aBSREL and PAML's M1a vs. M2a) some genes showed evidence of positive selection whether the species tree or gene tree was used. In contrast, many other genes had signatures of positive selection restricted only to a single specification strategy. As expected, genes that were sensitive to specification strategy tended to more discordant with the species tree, while the genes that showed evidence of positive selection regardless of the tree used had levels of discordance comparable to all genes (85%, Figure 6, numbers in parentheses). This suggests that specifying a potentially incorrect tree (*e.g.*, the species tree when the underlying gene trees are discordant) can often affect inferences of positive selection. The magnitude and direction of these biases were dependent on the underlying model. So-called branch-site models that allow substitution rates to vary among both branches and codon sites, such as HyPhy's BUSTED and aBSREL models, resulted in more genes inferred with evidence for positive selection when using the local gene tree. This suggests that using a single species tree for branch-site tests may reduce the power to detect positive selection. On the other hand, models that only allow rates to vary among sites, such as PAML's M1a vs. M2a test, showed an increase in the number of cases where there was positive selection detected with the species trees but not with the local gene tree. As these inferences are based on empirical data, the actual phylogenetic histories are not known and both specification strategies could result in errors. That said, our findings suggest that phylogenetic discordance may bias results towards spurious increases in d_N/d_S that mimics positive directional selection in some instances, or loss of power to detect selection in other cases and that the magnitude and direction of these biases vary by model type.

These results have wide-ranging implications for phylogenetics and comparative genomic analysis. First, it is imperative that when testing a specific locus for positive selection, discordance among loci must be accounted for. This is most easily achieved by simply using the gene tree (or other locus type) as input to the test for selection (Good, et al. 2013; Mendes and Hahn 2016; Roycroft, et al. 2021). However, as Mendes and Hahn (2016) pointed out, this may not completely mask the effects of discordance on substitution rates, as sites within a single gene may still have evolved under different histories because of within-gene recombination. Indeed, we found that tree similarity diminished at scales that were less than the average genomic distance between the beginning and end of a coding sequence in mice (~37 kb in this data set). Nevertheless, we suggest that starting with an inferred gene tree is advisable whenever possible, followed by a secondary analysis of evidence for within-gene variation in phylogenetic history. Our results also imply that studies of molecular evolution may benefit from approaches that reduce genome-wide levels of discordance, such as through *post hoc* pruning of species that disproportionately contribute to unresolved nodes.

Incorporating discordance into a comparative framework is not trivial and many comparative genomic methods assume a single species tree that test for changes in substitution rates in a phylogeny (Pollard, et al. 2010; Hu, et al. 2019; Partha, et al. 2019). Even methods that allow the use of different trees for different loci (like PAML and HyPhy) are still commonly applied with a single species tree across loci (Carbone, et al. 2014; Foote, et al. 2015; van der Valk, et al. 2021; Treaster, et al. 2023). Our suggestions are on the simple assumption that the results from the local gene tree are more likely to be correct, but, as noted above, this may not always be the case given that errors can also occur during gene tree inference. Still, our results confirm that the use of a single tree for all loci for such tests that rely on accurate estimation of substitution rates are likely to lead to both inaccurate inferences of positive selection. We strongly encourage the use of individual gene trees for such analyses.

Conclusions

Murine rodents as a study system allow us to use the high-quality *M. musculus* genome to examine fine-scale patterns and effects of phylogenetic discordance along chromosomes. Our analysis reveals how discordance varies with genome biology across evolutionary timescales, as well as the limits of inference inherent to extrapolating information from a single model system to a phylogenetic sample. We also demonstrate how phylogenetic discordance can mislead common tests for selection if only a single species tree is used. Overall, our results emphasize that progress in comparative genomics requires a detailed understanding of the heterogeneous biological signals in phylogenomic datasets.

Our results help illuminate the complexities of phylogenomic datasets and the need to accommodate phylogenetic discordance in genome-wide analyses. Genomic data now dominate the study of both population genetics and phylogenetics, and these once disparate fields are increasingly unified. Species tree phylogenies are an emergent pattern of the genome-wide accumulation of stochastic and directional population-level processes that cannot be fully captured or modeled by a single history (Steenwyk, et al. 2023). Importantly, phylogenetic discordance is not limited to closely related populations or species and is expected to leave persistent signals over deep evolutionary timescales (Oliver 2013). In turn, the use of tree-based frameworks for studying evolution (at any timescale) must incorporate the population-level processes that shape phylogenetic discordance. There appear to be relatively few tree-based applications where the use of a single evolutionary history is appropriate. Indeed, failure to account for phylogenetic discordance can lead to spurious inferences of molecular evolution (Figure 6; Mendes, et al. (2016)), trait evolution (Avise and Robinson 2008; Hahn and Nakhleh 2016), and even species diversification (Louca and Pennell 2020). Similar to the need for robust baseline models in population genomic inference (Johri, et al. 2022), understanding the causes and landscape of phylogenetic discordance constitutes a critical first step in phylogenomic analysis (Mirarab, et al. 2021; Steenwyk, et al. 2023).

Materials & Methods

Sample collection and assembly

We collected genomes from 16 murine species and two other rodents from several sources, including NCBI and several recently sequenced in Kumon, et al. (2021) (see Table S1 for full list of samples and sources). We also report the genome of *Otomys typus* (FMNH 230007) from Ethiopia in 2015. While DNA extraction and sequencing on the 10x Genomics platform for *O. typus* is the same as described in (Kumon, et al. 2021), the library quality for this sample was too low for chromosome level assembly. Here, we instead assembled it into scaffolds with the express purpose of obtaining UCEs for phylogenetic analysis. Adapters and low-quality bases were trimmed from the reads using illumiprocessor (Faircloth 2013), which makes use of functions from trimmomatic (Bolger, et al. 2014). All cleaned reads were de novo assembled using ABySS 2.3.1 (Jackman, et al. 2017) with a Bloom filter (Bloom 1970) de Bruijn graph. The final *O. typus* scaffold assembly was 2.14GB (N50=9,211; L50=64,014; E-size=12,790).

In parallel, for six of these species (see Figure 1; Table S1), we generated reference-based pseudo-assemblies with iterative mapping using an updated version pseudo-it v3.1.1 (Sarver, et al. 2017) that incorporates insertion-deletion variation to minimize reference bias in our genome-wide phylogenetic analyses and to maintain collinearity between assemblies (<https://github.com/goodest-goodlab/pseudo-it>). We used the *Mus musculus* (mm10) genome as the reference for our pseudo-assembly approach. Briefly, pseudo-it maps reads from each sample to the reference genome with BWA (Li 2013), calls variants with GATK HaplotypeCaller (Poplin, et al. 2018), and filters SNPs and indels and generates a consensus assembly with bcftools (Danecek, et al. 2021). The process is repeated, each time using the previous iteration's consensus assembly as the new reference genome to which reads are mapped. In total, we did three iterations of mapping for each sample.

Ultraconserved element (UCE) retrieval and alignment

We first set out to reconstruct a phylogeny of sequenced murine rodents to provide both a general resource for future comparative genomic studies within this important group as well as a time-calibrated phylogeny to frame an in-depth analysis of phylogenetic discordance across a subset of murine whole genomes (see below). We combined our seven recently sequenced genomes with nine publicly available murine genomes as well as the genomes of two non-murine rodents, the great gerbil (*Rhombomys opimus*; Nilsson, et al. 2020) and the Siberian hamster (*Phodopus sungorus*; Moore, et al. 2022) as outgroups. We extracted UCEs from each species, plus 1000 flanking bases from each side of the element using the protocols for harvesting loci from genomes and the *M. musculus* UCE probe set provided with phyluce v1.7.1 (Faircloth, et al. 2012; Faircloth 2016). In total, we recovered 2,632 unique UCE loci, though not all UCE loci were found in all taxa (Table S1).

We brought the extracted UCE sequences for each species into a consistent orientation using MAFFT v7 (Katoh and Standley 2013) and then aligned them using FSA (Bradley, et al. 2009) with the default settings. We trimmed UCE alignments with TrimAl (Capella-Gutierrez, et

al. 2009) with a gap threshold of 0.5 and otherwise default parameters. We performed alignment quality checks using AMAS (Borowiec 2016). We processed all alignments in parallel with GNU Parallel (Tange 2018).

Species tree reconstruction from UCEs

We constructed a species-level rodent phylogeny with two approaches. First, using the alignments of all UCEs found in four or more taxa (2,632), we reconstructed a maximum-likelihood (ML) species tree with IQ-TREE v2.2.1 (Minh, et al. 2020b). Each UCE alignment was concatenated and partitioned (Chernomor, et al. 2016) such that optimal substitution models were inferred for individual UCE loci with ModelFinder (Kalyaanamoorthy, et al. 2017). We also reconstructed individual gene trees for each UCE alignment. For all IQ-TREE runs (concatenated or individual loci), we assessed branch support with ultrafast bootstrap approximation (UFBoot) (Hoang, et al. 2018) and the corrected approximate likelihood ratio test (SH-aLRT) (Guindon, et al. 2010). We collapsed branches in each UCE tree exhibiting less than 10% approximated bootstrap support using the `nw_ed` function from Newick Utilities (Junier and Zdobnov 2010). We used these trees as input to the quartet summary method ASTRAL-III v5.7.8 (Zhang, et al. 2018) to infer a species tree. We generated visualizations of phylogenies with R v4.1.1 (R Core Team 2021) using `phytools` v1.9-16 (Revell 2012) and the `ggtree` package v3.14 (Yu, et al. 2017; Yu 2020) and its imported functions from `ape` v5.0 (Paradis and Schliep 2019) and `treeio` v1.16.2 (Wang, et al. 2020).

We then used two methods to assess phylogenetic discordance across the reconstructed species tree. First, we calculated site and gene concordance factors (sCF and gCF) with IQ-TREE 2 (Minh, et al. 2020a; Minh, et al. 2020b) to assess levels of phylogenetic discordance between the inferred UCE trees and the concatenated species tree. gCF is calculated for each branch in the species tree as the proportion of UCE trees in which that branch also appears (Baum 2007). sCF represents the proportion of alignment sites concordant with a given species tree branch in a randomized subset of quartets of taxa (Minh, et al. 2020a). We visualized gCF and sCF (Lanfear 2018) for each branch in each species tree using methods in R v4.3.0 (Lanfear 2018; R Core Team 2021). Next, we used PhyParts (Smith, et al. 2015b) to identify topological conflict between the UCE trees and the species tree from ASTRAL-III. For this analysis, we rooted all trees with *Phodopus sungorus* as the outgroup using the `nw_reroot` function in the Newick Utilities (Junier and Zdobnov 2010) package and excluded 204 UCE trees that did not contain the outgroup.

Divergence time estimation

We used IQ-TREE 2's (Minh, et al. 2020b) implementation of least square dating to estimate branch lengths of our species trees in units of absolute time (To, et al. 2016). To improve divergence-time estimation, we used SortaDate (Smith, et al. 2018) to identify a set of 100 UCE loci that exhibit highly clocklike behavior and minimized topological conflict with the concatenated species tree. We applied four node age calibrations (Table S3) as described in Kimura, et al. (2015) and Aghova, et al. (2018). The origin of core Murinae (Node E) was

constrained to between 11.1 and 12.3 Ma, following Kimura, et al. (2015). Maximum ages were set for Otomyini+Arvicanthini (9.2 Ma, Kimura, et al. 2015), *Apodemus* (9.6 Ma, Daxner-Höck 2002), and *Mus* (8.0 Ma, Kimura, et al. 2013). Branch lengths were resampled 100 times to produce confidence intervals.

Genome window-based phylogenetic analysis

For the second part of our work, we wanted to quantitatively infer phylogenetic discordance across a subset of the murine genomes used to infer the species tree and relate that discordance to other features of the genome, such as recombination rate, proximity to genes, and rates of molecular evolution. To assess the distribution of phylogenetic discordance across rodent genomes, we limited subsequent analyses to *M. musculus* and the pseudo-assemblies (see above) of six of the genomes (*Mastomys natalensis*, *Hylomyscus alleni*, *Praomys delectorum*, *Rhabdomys dilectus*, *Grammomys dolichurus*, and *Rhynchomys soricoides*). *Otomys typus* was excluded from these analyses due to the inadequacy of the library outlined above.

We partitioned these genomes into 10 kilobase (kb) windows based on the coordinates in the reference *M. musculus* genome (mm10; Mouse Genome Sequencing, et al. 2002) using bedtools makewindows (Quinlan and Hall 2010). These coordinates were converted between the reference and the consensus sequence for each genome using liftOver (Hinrichs, et al. 2006). Note that this method assumes both collinearity of all genomes and similar karyotypes (see Discussion). We then removed windows from the subsequent analyses if (1) 50% or more of the window overlapped with repeat regions from the *M. musculus* reference RepeatMasker (Smit, et al. 2013-2015) file downloaded from the UCSC Genome Browser's table browser (Hinrichs, et al. 2006) or (2) 50% or more of the window contained missing data in three or more samples. Overlaps with repeat regions were determined with bedtools coverage (Quinlan and Hall 2010). We then aligned the 10kb windows with MAFFT (Katoh and Standley 2013), trimmed alignments with trimAl (Capella-Gutierrez, et al. 2009), and inferred phylogenies for each with IQ-TREE 2 (Minh, et al. 2020b) which uses ModelFinder to determine the best substitution model for each window (Kalyaanamoorthy, et al. 2017).

To assess patterns of tree similarity between windows on the same chromosome, we used the weighted Robinson-Foulds (wRF) (Robinson and Foulds 1981; Böcker, et al. 2013) distance measure implemented in the phangorn library (Schliep 2011) in R (R Core Team 2021), which compares two trees by finding clades or splits present in one tree but not the other weighted by the missing branch length in each tree for each mismatch and differences in branch length between the co-occurring branches in both trees (Robinson and Foulds 1979). Consequently, the resulting measure of wRF is in units of branch length (i.e., expected number of substitutions per site for maximum likelihood trees). We compared wRF between trees from windows on the same chromosome to characterize (1) heterogeneity in patterns discordance along the chromosome and (2) whether tree similarity is correlated with distance between windows. For the second question, we sampled every window on a chromosome at increasing distance (in 10kb windows) until the distribution of wRF scores for all pairs of windows at that distance was not significantly different

(Wilcox test, $p > 0.01$) than that of a sample of 12,000 measures of wRF between randomly selected trees on different chromosomes. We selected 12,000 as the random sample size because it roughly matched the number of windows on the largest chromosome (chromosome 1, $n = 12,113$). We used Snakemake 7 (Mölder, et al. 2021) to compute window alignments and trees in parallel.

Whole genome alignment between mouse and rat

To assess how un-accounted for large-scale structural variation may impact our conclusions, we compared the reference mouse and rat genomes. We used minimap2 (Li 2018) to align the mouse (mm10) and rat (rnor6) (Gibbs, et al. 2004) genomes to assess the impact of structural variation that spans the divergence of our subset of species used in the discordance analyses. We downloaded the rat reference genome (rnor6) from the UCSC genome browser and for both genomes removed the Y chromosome and all smaller unplaced scaffolds. We then used minimap2 in whole genome alignment mode (-x asm20) to generate a pairwise alignment file from which we calculated alignment segment sizes and the distances between alignment segments. We visualized the alignment as a dot plot using the pafr package in R (<https://github.com/dwinter/pafr>).

Recombination rate and functional annotation

We retrieved 10,205 genetic markers generated from a large heterogenous stock of outbred mice (Shifman, et al. 2006; Cox, et al. 2009) to assess whether phylogenetic discordance along chromosomes was correlated with mouse recombination rates. We converted the physical coordinates of these markers from build 37 (mm9) to build 38 (mm10) of the *M. musculus* genome using liftOver (Hinrichs, et al. 2006). We then partitioned the markers into 5Mb windows and estimated local recombination rates defined as the slope of the correlation between the location on the *M. musculus* genetic and physical maps for all markers in the window (White, et al. 2009; Kartje, et al. 2020). Within each 5Mb window, we calculated wRF distances between the first 10kb window and every other 10kb window.

We also compared the chromosome-wide wRF distances to those based on phylogenies from regions around several types of adjacent to genomic features. We retrieved coordinates from 25,753 protein coding genes annotated in *M. musculus* from Ensembl (release 99; Cunningham, et al. 2022), all 3,129 UCEs from the *M. musculus* UCE probe set provided with PHYLUCE (Faircloth, et al. 2012; Faircloth 2016), and 9,865 recombination hotspots from Smagulova, et al. (2011). The recombination hotspot coordinates were converted between build 37 and build 38 using the liftOver tool (Hinrichs, et al. 2006). For each feature, the starting window was the 10kb window containing the feature's midpoint coordinate. We then calculated wRF between this window and all windows within 5Mb in either direction and for each chromosome compared the slope and wRF distance of windows adjacent to the feature with the same metrics for the whole chromosome. We compared distributions of these measures for each genomic feature with an ANOVA (`aov(feature.measure ~ feature.label)`) followed by Tukey's range test

(TukeyHSD(anova.result)) to assess differences in means, as implemented in R v4.1.1 (R Core Team 2021).

Molecular evolution

To test how tree misspecification affects common model-based analyses of molecular evolution, we retrieved 22,261 coding sequences from *M. musculus* using the longest coding transcript of each gene. Coding coordinates from the *M. musculus* coding sequences were transposed to the new assemblies via liftOver (Hinrichs, et al. 2006) and sequences retrieved with bedtools getfasta (Quinlan and Hall 2010). We recovered 17,216 genes that were present in all seven species. Using MACSE (Ranwez, et al. 2018), we trimmed non-homologous regions from each ortholog using trimNonHomologousFragments, aligned the orthologs using alignSequences, and trimmed the aligned sequences with trimAlignment to remove unaligned flanking regions. Finally, we manually filtered the alignments using the following (non-mutually exclusive) criteria: 3,368 alignments were removed during filtering for gapped sites, 3,132 alignments had a premature stop codon in at least one species, 1,571 alignments had only three or fewer unique sequences among the seven species, and 78 alignments were shorter than 100 bp. After filtering, 12,559 total alignments for tree reconstruction and inference of selection.

We then used IQ-TREE 2 (Minh, et al. 2020b) to reconstruct a single species tree from concatenation of all gene alignments, as well as gene-trees for each individual alignment. This species tree from coding regions matches the topologies of these species inferred by concatenation of UCEs in the previous section. Next we ran several tests that use both coding alignments and a tree to infer positive selection: PAML's M1a vs. M2a test (Yang 2007), HyPhy's aBSREL model (Smith, et al. 2015a), and HyPhy's BUSTED model (Murrell, et al. 2015). We ran each test twice on each gene, once using the species tree derived from concatenated data, and once using the tree estimated for that gene. For the HyPhy models, no target branch was selected, meaning all branches in the input phylogeny were tested.

The end point of each of these three tests is a p-value, which lets us assess whether a model that allows for positively selected sites fits better than a model that does not. For M1a vs. M2a, we obtained the p-value manually by first performing a likelihood ratio test to determine genes under selection by calculating $2 * (lnl M1a - lnl M2a)$. The p-value of this likelihood ratio is then retrieved from a one-tailed chi-square distribution with two degrees of freedom (Yang 2007). For BUSTED and aBSREL, p-values are computed automatically during the test using similar likelihood ratios. For the M1a vs. M2a and BUSTED tests, a single p-value is computed for each gene. P-values were adjusted by correcting for false discovery rates (Benjamini and Hochberg 1995; Yekutieli and Benjamini 1999) using the "fdr" method in the p.adjust() function in R (R Core Team 2021) and we categorized a gene as being positively selected if its adjusted p-value was < 0.01 . For the aBSREL test, a p-value is generated for each branch in the input gene tree. aBSREL corrects for multiple testing internally across branches using the Holm-Bonferroni procedure (Holm 1979; Pond, et al. 2005). We further correct the p-values across genes with the Bonferroni method and classify a gene as having experienced positive selection if one or more

branches has a p-value < 0.01 after all corrections. We used Snakemake 7 (Mölder, et al. 2021) to compute coding alignments, trees, and selection tests in parallel.

Data availability

For the six previously assembled genomes (see Table S1), all raw reads and assemblies are available as an NCBI BioProject (Accession Number PRJNA669840). The reads and assembly for *Otomys* typus, pseudo-assemblies for the six other new samples, and locus alignments (UCEs, genes, and genomic windows) are available on Dryad (<https://doi.org/10.5061/dryad.866t1glwq>). All code and summary data for this project are deposited on github (<https://github.com/gwct/murine-discordance>).

Acknowledgments

We thank Jake Esselstyn and Kevin Rowe for helpful comments and discussion on the murine species tree and Matt Hahn and the Hahn lab for feedback on the manuscript. We also thank Brant Faircloth and Trevor Sless for advice on using phyluce. We are grateful for tissue samples provided by Chris Conroy at the Museum of Vertebrate Zoology, Berkeley, CA (MVZ) and Adam Ferguson at the Field Museum of Natural History, Chicago, IL (FMNH), and to the original collectors. This work was supported by the National Science Foundation (DEB-1754096 to J.M.G.), the Eunice Kennedy Shriver National Institute of Child Health and Human Development of the National Institutes of Health (R01-HD094787 to J.M.G.). J.J.H. received financial support from the Cornell Center for Vertebrate Genomics. J.S.B. was supported by the University of Michigan Life Sciences Fellows Program and the Jean Wright Cohn Endowment Fund at the University of Michigan Museum of Zoology. Computations for species tree reconstruction were performed using the computer clusters and data storage resources of the University of California Riverside HPCC, which were funded by grants from NSF (MRI-2215705, MRI-1429826) and NIH (1S10OD016290-01A1), and the Cornell University Biotechnology Resource Center BioHPC (RRID:SCR_021757) with help from Qi Sun. Bioinformatic analyses for genomic discordance and selection tests were conducted using the University of Montana Griz Shared Computing Cluster supported by grants from the NSF (CC-2018112 and OAC-1925267, J.M.G. co-PI). Any opinions, findings, and conclusions or recommendations expressed in this material are those of the authors and do not necessarily reflect the views of the NSF or the NIH.

719 **Tables**

720 **Table 1. Incidence where a single species tree does not match the gene tree expectation in**
 721 **three different tests for positive selection, either not detecting positive selection when it is**
 722 **inferred using the gene tree (Undetected selection) or by detecting positive selection that is**
 723 **not inferred when using the gene tree (Newly detected selection).**

Test	Undetected selection	Newly detected selection
BUSTED	0.45%	28.10%
aBSREL	0.41%	10.60%
M1a vs. M2a	2.66%	3.20%

724

Figures

Figure 1

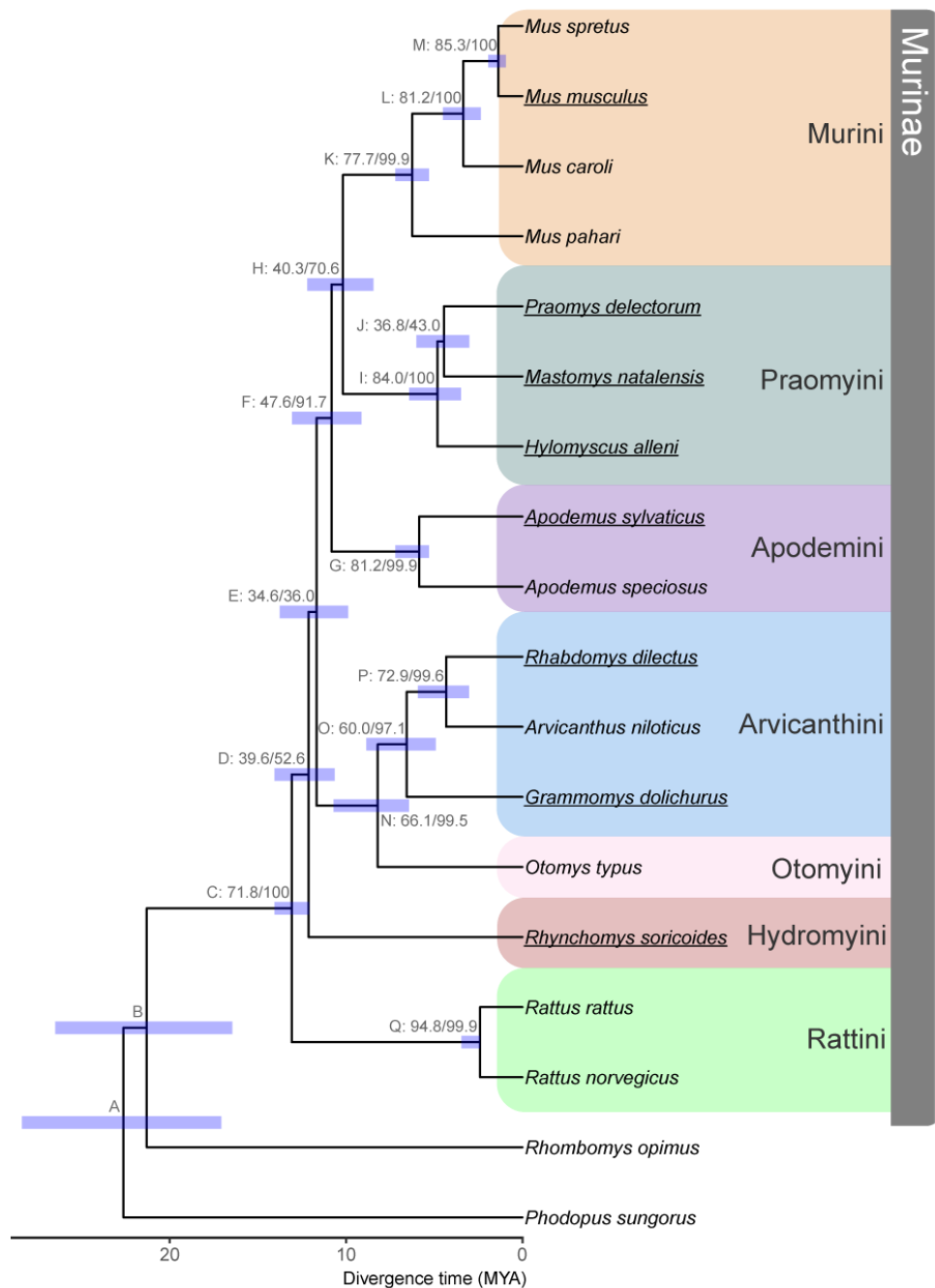
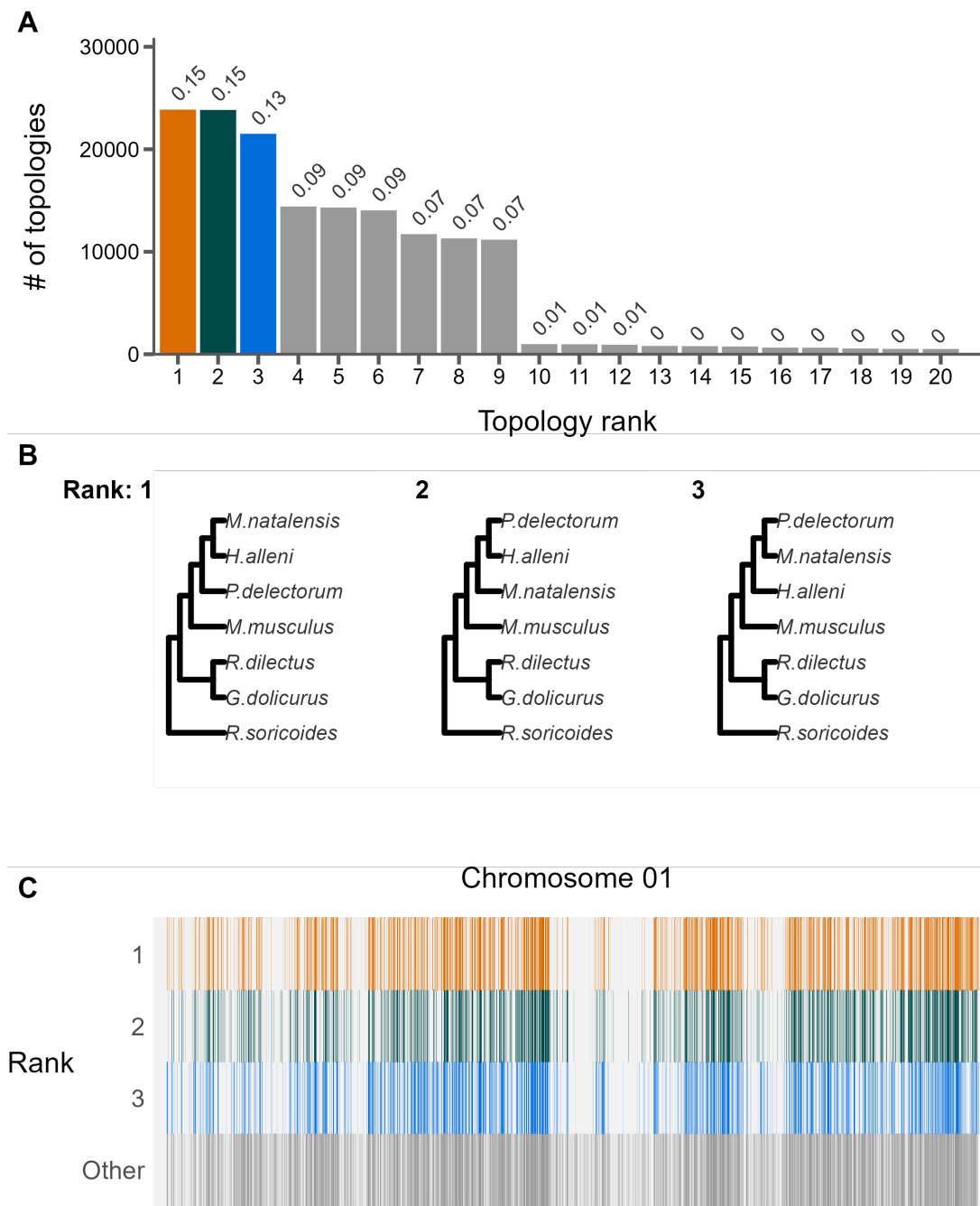


Figure 1. Species trees inferred from concatenation of ultra-conserved elements (UCEs) from 18 rodent species. Internal nodes are labeled by a letter identifier referenced in the text and site and gene concordance factors (*i.e.*, Label: sCF/gCF) as well as a bar indicating the confidence interval for divergence time estimation. Ultrafast bootstrap/SH-aLRT values were all 100. Bottom scale represents time in millions of years before present. Fossil calibrations are described in Tables S2

733 and S3. Tribes within sub-family Murinae are highlighted on the right following the classifications
734 used by Lecompte, et al. (2008). Genomes used for the genome-wide phylogenetic discordance
735 analyses are underlined.

736

737 **Figure 2**



738

739 **Figure 2.** The landscape and profile of phylogenetic discordance across non-overlapping 10kb
740 windows in murine genomes. A) Distribution of the 20 most frequent topologies recovered across
741 all windows. Numbers above bars indicate proportion of each topology. B) The top three
742 topologies recovered across all chromosomes 1. C) Distribution of the topologies recovered along

743 chromosome 1. The x-axis is scaled to the length of the chromosome and each vertical bar
744 represents one 10kb window. The three most frequent topologies occupy the first three rows while
745 all other topologies are shown in the bottom row. See Supplemental File S1 for individual
746 chromosome plots.

Figure 3

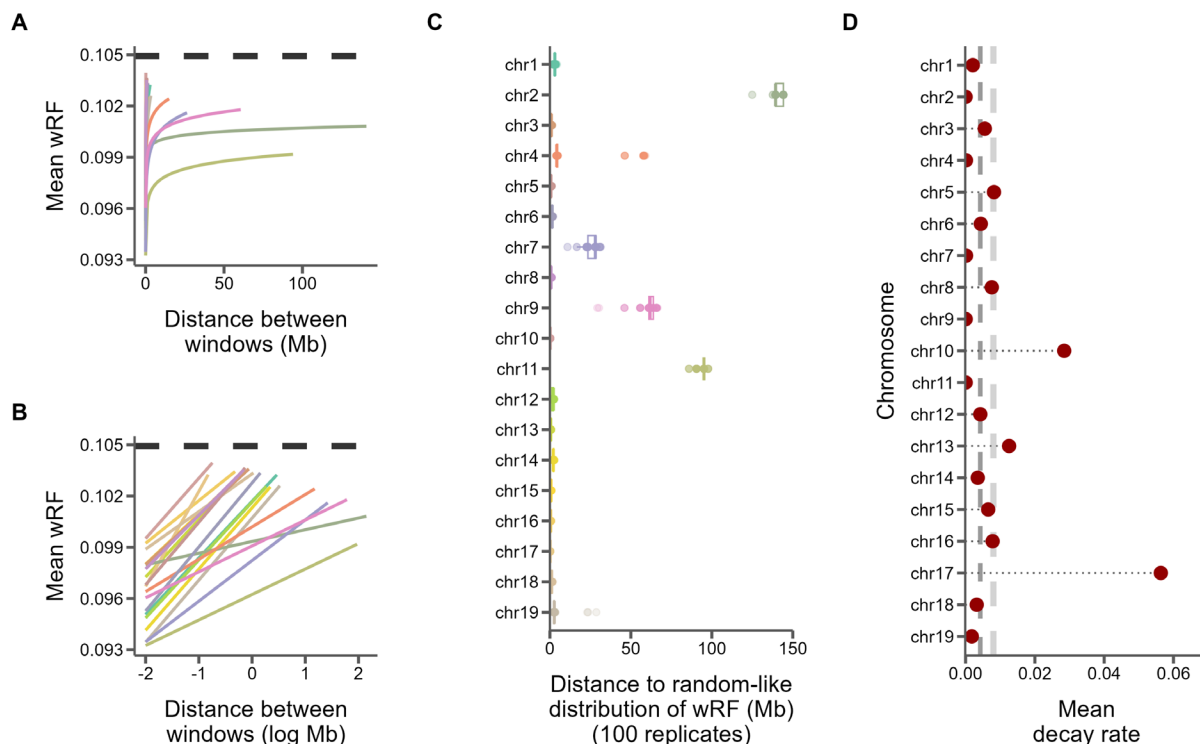


Figure 3. Similarity between 10kb windows decays as genomic distance between windows increases. A) The log fit to the mean of distributions of weighted Robinson-Foulds distances between trees of windows at increasing genomic distance (10kb steps). Each line represents one chromosome. B) The same, but on a log scale with a linear fit. C) For every window on each chromosome, the genomic distance between windows at which tree distance becomes random for 100 replicates of random window selection. D) Points represent the slopes of the correlation between genomic distance and tree distance (lines from panel B), which is the rate at which tree similarity decays across the genome. Dark grey dashed line is median slope and light grey dashed line is mean.

Figure 4

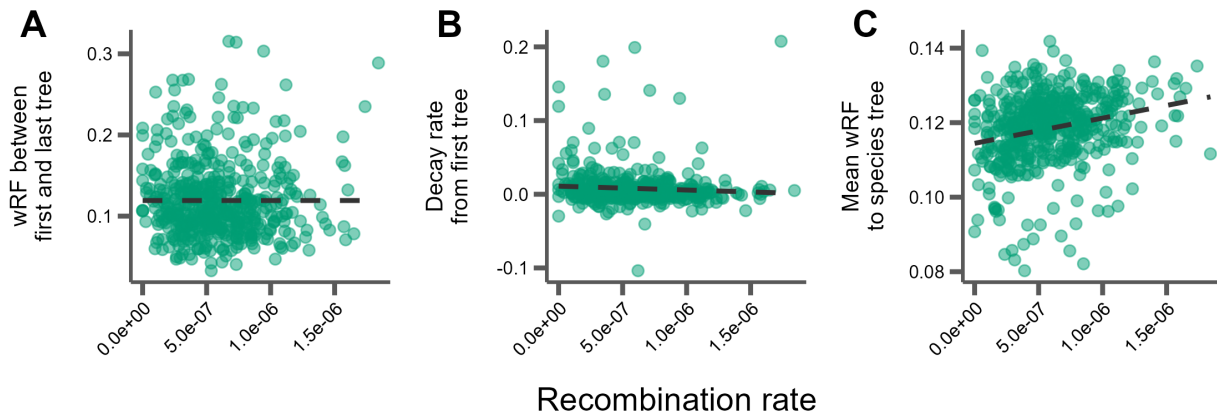
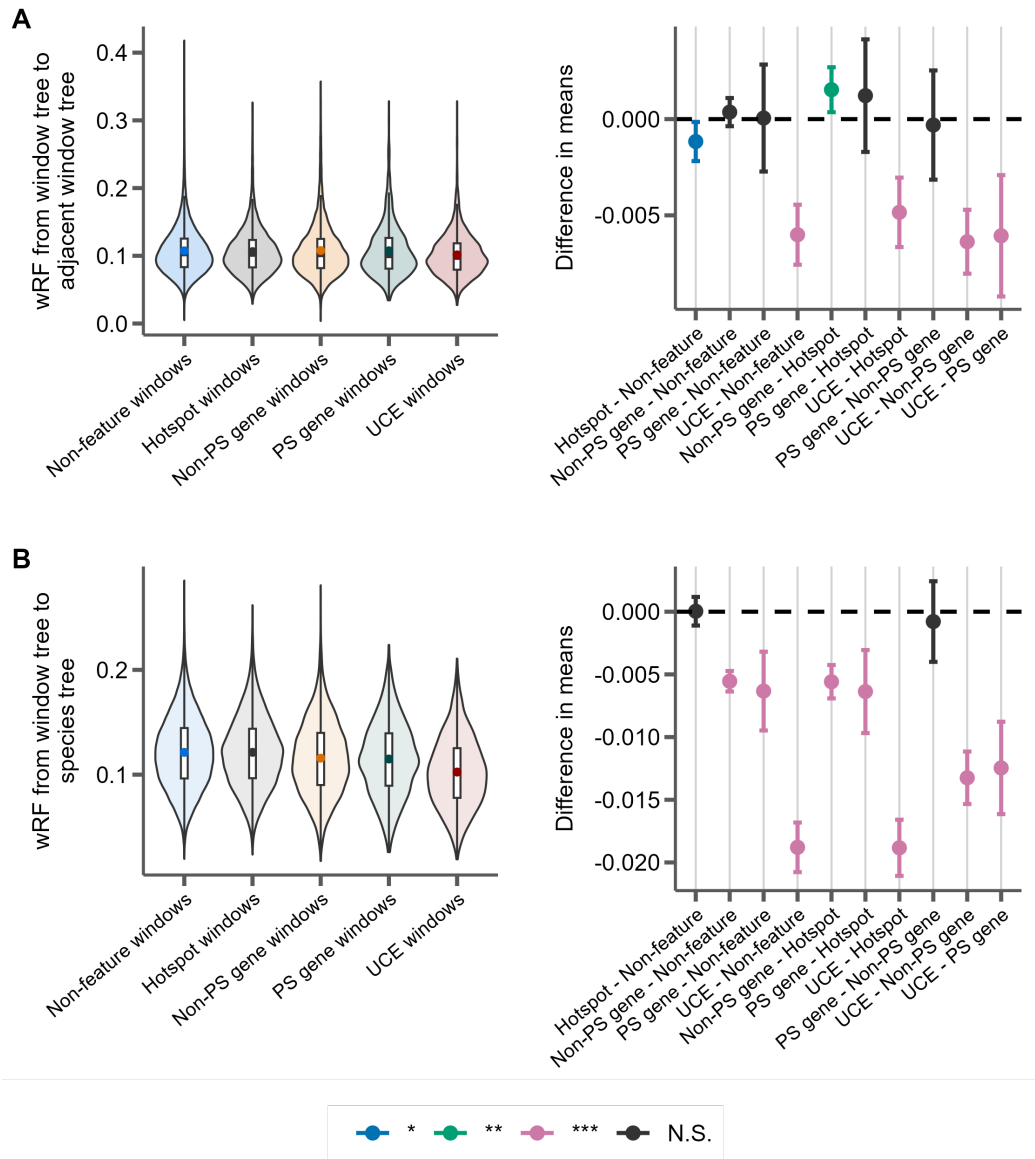


Figure 4. Correlations between tree similarity and recombination rate in 5 Mb windows. A) Tree similarity as measured by the weighted Robinson-Foulds distance between the first and last 10 kb windows within the 5 Mb window. B) The slopes of the linear correlation between the weighted Robinson-Foulds distances between the first 10 kb window and every other 10 kb window within a 5 Mb window represent the rate at which tree similarity decays over each 5 Mb window. C) The mean wRF of all 10 kb window trees within each 5Mb window compared to the species tree.



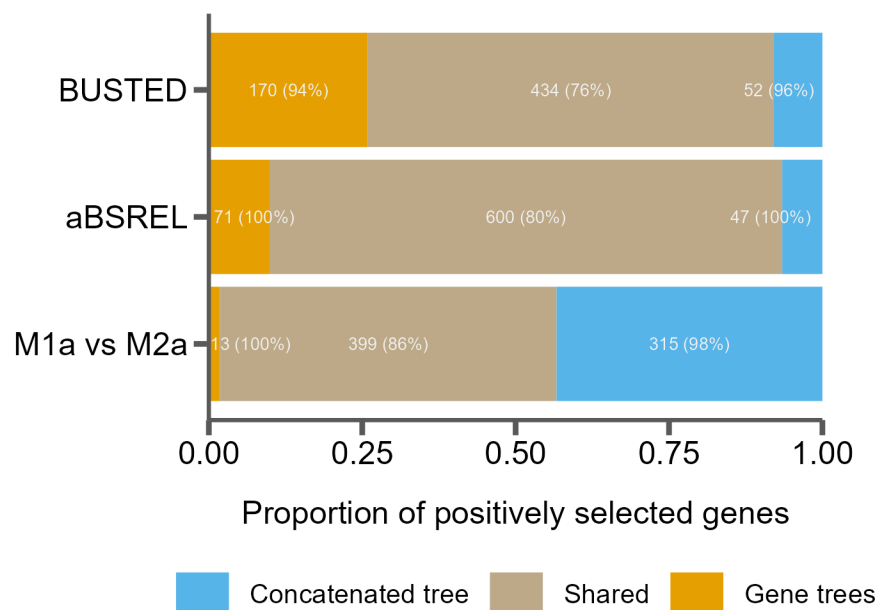
769

770 **Figure 5.** Distributions of weighted Robinson-Foulds distance from trees constructed from 10kb
771 windows either centered on recombination hotspots (Hotspot), protein-coding genes without
772 evidence for positive selection (Non-PS genes), protein coding genes with evidence for positive
773 selection (PS genes), UCEs, or containing none of these features (Non-feature). For each panel,
774 the left portion shows the distributions of the measure for each feature type and the right panel
775 shows the differences in means for each pairwise comparison of features with significance assessed
776 with Tukey's range test. The labels on the x-axis indicate the feature pairs being compared, with
777 the first feature being the reference (*i.e.* points above 0 indicate this feature has a higher mean). *P*-
778 value thresholds: * < 0.05, ** < 0.01, *** < 0.001. A) The phylogenetic similarity of windows

779 immediately adjacent to feature windows. B) The phylogenetic similarity between the species tree
780 inferred from protein-coding gene trees and the feature window.

781

782 **Figure 6**



783
784 **Figure 6.** The proportion of genes inferred to be under positive selection for three tests using either
785 a single species tree (concatenated tree) or individual gene trees, as well as those found in both
786 cases (shared). Numbers in the bars indicate raw counts, and percentages indicate the percent of
787 genes in that category that are discordant from the species tree.

788
789
790

References

- Aghova T, Kimura Y, Bryja J, Dobigny G, Granjon L, Kergoat GJ. 2018. Fossils know it best: Using a new set of fossil calibrations to improve the temporal phylogenetic framework of murid rodents (Rodentia: Muridae). *Mol Phylogenet Evol* 128:98-111.
- Alda F, Ludt WB, Elias DJ, McMahan CD, Chakrabarty P. 2021. Comparing Ultraconserved Elements and Exons for Phylogenomic Analyses of Middle American Cichlids: When Data Agree to Disagree. *Genome Biol Evol* 13:evab161.
- Alexander AM, Su YC, Oliveros CH, Olson KV, Travers SL, Brown RM. 2017. Genomic data reveals potential for hybridization, introgression, and incomplete lineage sorting to confound phylogenetic relationships in an adaptive radiation of narrow-mouth frogs. *Evolution* 71:475-488.
- Avise JC, Robinson TJ. 2008. Hemiplasy: a new term in the lexicon of phylogenetics. *Syst Biol* 57:503-507.
- Baudat F, Buard J, Grey C, Fledel-Alon A, Ober C, Przeworski M, Coop G, de Massy B. 2010. PRDM9 is a major determinant of meiotic recombination hotspots in humans and mice. *Science* 327:836-840.
- Baum DA. 2007. Concordance trees, concordance factors, and the exploration of reticulate genealogy. *TAXON* 56:417-426.
- Benjamini Y, Hochberg Y. 1995. Controlling the false discovery rate: a practical and powerful approach to multiple testing. *Journal of the Royal statistical society: series B (Methodological)* 57:289-300.
- Bloom BH. 1970. Space/time trade-offs in hash coding with allowable errors. *Commun. ACM* 13:422-426.
- Böcker S, Canzar S, Gunnar WK. 2013. The Generalized Robinson-Foulds Metric. In: Darling A, Stoye J, editors. *Algorithms in Bioinformatics*. Berlin, Heidelberg: Springer.
- Bolger AM, Lohse M, Usadel B. 2014. Trimmomatic: a flexible trimmer for Illumina sequence data. *Bioinformatics* 30:2114-2120.
- Borowiec ML. 2016. AMAS: a fast tool for alignment manipulation and computing of summary statistics. *PeerJ* 4:e1660.

829
830 Bradley RK, Roberts A, Smoot M, Juvekar S, Do J, Dewey C, Holmes I, Pachter L. 2009. Fast
831 statistical alignment. *PLoS Comput Biol* 5:e1000392.

832
833 Capella-Gutierrez S, Silla-Martinez JM, Gabaldon T. 2009. trimAl: a tool for automated alignment
834 trimming in large-scale phylogenetic analyses. *Bioinformatics* 25:1972-1973.

835
836 Carbone L, Harris RA, Gnerre S, Veeramah KR, Lorente-Galdos B, Huddleston J, Meyer TJ,
837 Herrero J, Roos C, Aken B, et al. 2014. Gibbon genome and the fast karyotype evolution of small
838 apes. *Nature* 513:195-201.

839
840 Chan KO, Hutter CR, Wood PL, Jr., Grismer LL, Brown RM. 2020. Target-capture phylogenomics
841 provide insights on gene and species tree discordances in Old World treefrogs (Anura:
842 Rhacophoridae). *Proc Biol Sci* 287:20202102.

843
844 Charlesworth B, Morgan MT, Charlesworth D. 1993. The effect of deleterious mutations on
845 neutral molecular variation. *Genetics* 134:1289-1303.

846
847 Chernomor O, von Haeseler A, Minh BQ. 2016. Terrace Aware Data Structure for Phylogenomic
848 Inference from Supermatrices. *Syst Biol* 65:997-1008.

849
850 Christmas MJ, Kaplow IM, Genereux DP, Dong MX, Hughes GM, Li X, Sullivan PF, Hindle AG,
851 Andrews G, Armstrong JC, et al. 2023. Evolutionary constraint and innovation across hundreds of
852 placental mammals. *Science* 380:eabn3943.

853
854 Cox A, Ackert-Bicknell CL, Dumont BL, Ding Y, Bell JT, Brockmann GA, Wergedal JE, Bult C,
855 Paigen B, Flint J, et al. 2009. A new standard genetic map for the laboratory mouse. *Genetics*
856 182:1335-1344.

857
858 Cunningham F, Allen JE, Allen J, Alvarez-Jarreta J, Amode MR, Armean IM, Austine-Orimoloye
859 O, Azov AG, Barnes I, Bennett R, et al. 2022. Ensembl 2022. *Nucleic Acids Res* 50:D988-D995.

860
861 Danecek P, Bonfield JK, Liddle J, Marshall J, Ohan V, Pollard MO, Whitwham A, Keane T,
862 McCarthy SA, Davies RM, Li H. 2021. Twelve years of SAMtools and BCFtools. *Gigascience*
863 10:giab008.

864
865 Dapper AL, Payseur BA. 2017. Connecting theory and data to understand recombination rate
866 evolution. *Philos Trans R Soc Lond B Biol Sci* 372.

Daxner-Höck G. 2002. *Cricetodon meini* and other rodents from Mühlbach and Grund, Lower Austria (Middle Miocene, late MN5). *Annalen des Naturhistorischen Museums in Wien. Serie A für Mineralogie und Petrographie, Geologie und Paläontologie, Anthropologie und Prähistorie*:267-291.

Degnan JH, Rosenberg NA. 2006. Discordance of species trees with their most likely gene trees. *PLoS Genet* 2:e68.

Edwards SV. 2009. Is a new and general theory of molecular systematics emerging? *Evolution* 63:1-19.

Faircloth BC. 2013. illumiprocessor: a trimmomatic wrapper for parallel adapter and quality trimming.

Faircloth BC. 2016. PHYLUCE is a software package for the analysis of conserved genomic loci. *Bioinformatics* 32:786-788.

Faircloth BC, McCormack JE, Crawford NG, Harvey MG, Brumfield RT, Glenn TC. 2012. Ultraconserved elements anchor thousands of genetic markers spanning multiple evolutionary timescales. *Syst Biol* 61:717-726.

Feng S, Bai M, Rivas-Gonzalez I, Li C, Liu S, Tong Y, Yang H, Chen G, Xie D, Sears KE, et al. 2022. Incomplete lineage sorting and phenotypic evolution in marsupials. *Cell* 185:1646-1660 e1618.

Ferreira MS, Jones MR, Callahan CM, Farelo L, Tolesa Z, Suchentrunk F, Boursot P, Mills LS, Alves PC, Good JM, Melo-Ferreira J. 2021. The Legacy of Recurrent Introgression during the Radiation of Hares. *Syst Biol* 70:593-607.

Foley NM, Harris AJ, Bredemeyer KR, Ruedi M, Puechmaille SJ, Teeling EC, Criscitiello MF, Murphy WJ. 2024. Karyotypic stasis and swarming influenced the evolution of viral tolerance in a species-rich bat radiation. *Cell Genom* 4:100482.

Foley NM, Mason VC, Harris AJ, Bredemeyer KR, Damas J, Lewin HA, Eizirik E, Gatesy J, Karlsson EK, Lindblad-Toh K, et al. 2023. A genomic timescale for placental mammal evolution. *Science* 380:eabl8189.

905 Fontaine MC, Pease JB, Steele A, Waterhouse RM, Neafsey DE, Sharakhov IV, Jiang X, Hall AB,
 906 Catteruccia F, Kakani E, et al. 2015. Mosquito genomics. Extensive introgression in a malaria
 907 vector species complex revealed by phylogenomics. *Science* 347:1258524.

908
 909 Foote AD, Liu Y, Thomas GW, Vinar T, Alföldi J, Deng J, Dugan S, van Elk CE, Hunter ME,
 910 Joshi V, et al. 2015. Convergent evolution of the genomes of marine mammals. *Nat Genet* 47:272-
 911 275.

912
 913 Gable SM, Byars MI, Literman R, Tollis M. 2022. A Genomic Perspective on the Evolutionary
 914 Diversification of Turtles. *Syst Biol* 71:1331-1347.

915
 916 Gibbs RA, Weinstock GM, Metzker ML, Muzny DM, Sodergren EJ, Scherer S, Scott G, Steffen
 917 D, Worley KC, Burch PE, et al. 2004. Genome sequence of the Brown Norway rat yields insights
 918 into mammalian evolution. *Nature* 428:493-521.

919
 920 Good JM, Wiebe V, Albert FW, Burbano HA, Kircher M, Green RE, Halbwax M, Andre C,
 921 Atencia R, Fischer A, Paabo S. 2013. Comparative population genomics of the ejaculate in humans
 922 and the great apes. *Mol Biol Evol* 30:964-976.

923
 924 Green RE, Krause J, Briggs AW, Maricic T, Stenzel U, Kircher M, Patterson N, Li H, Zhai W,
 925 Fritz MH, et al. 2010. A draft sequence of the Neandertal genome. *Science* 328:710-722.

926
 927 Guindon S, Dufayard JF, Lefort V, Anisimova M, Hordijk W, Gascuel O. 2010. New algorithms
 928 and methods to estimate maximum-likelihood phylogenies: assessing the performance of PhyML
 929 3.0. *Syst Biol* 59:307-321.

930
 931 Hahn MW, Nakhleh L. 2016. Irrational exuberance for resolved species trees. *Evolution* 70:7-17.

932
 933 He B, Zhao Y, Su C, Lin G, Wang Y, Li L, Ma J, Yang Q, Hao J. 2023. Phylogenomics reveal
 934 extensive phylogenetic discordance due to incomplete lineage sorting following the rapid radiation
 935 of alpine butterflies (Papilionidae: Parnassius). *Syst Entomol*.

936
 937 Hibbins MS, Breithaupt LC, Hahn MW. 2023. Phylogenomic comparative methods: Accurate
 938 evolutionary inferences in the presence of gene tree discordance. *Proc Natl Acad Sci U S A*
 939 120:e2220389120.

940
 941 Hinrichs AS, Karolchik D, Baertsch R, Barber GP, Bejerano G, Clawson H, Diekhans M, Furey
 942 TS, Harte RA, Hsu F, et al. 2006. The UCSC Genome Browser Database: update 2006. *Nucleic*
 943 *Acids Res* 34:D590-598.

944
 945 Hoang DT, Chernomor O, von Haeseler A, Minh BQ, Vinh LS. 2018. UFBoot2: Improving the
 946 Ultrafast Bootstrap Approximation. *Mol Biol Evol* 35:518-522.

947
 948 Hobolth A, Christensen OF, Mailund T, Schierup MH. 2007. Genomic relationships and speciation
 949 times of human, chimpanzee, and gorilla inferred from a coalescent hidden Markov model. *PLoS*
 950 *Genet* 3:e7.

951
 952 Holm S. 1979. A simple sequentially rejective multiple test procedure. *Scandinavian journal of*
 953 *statistics*:65-70.

954
 955 Hu Z, Sackton TB, Edwards SV, Liu JS. 2019. Bayesian Detection of Convergent Rate Changes
 956 of Conserved Noncoding Elements on Phylogenetic Trees. *Mol Biol Evol* 36:1086-1100.

957
 958 Hudson RR. 1983. Testing the Constant-Rate Neutral Allele Model with Protein Sequence Data.
 959 *Evolution* 37:203-217.

960
 961 Hudson RR, Kaplan NL. 1988. The coalescent process in models with selection and
 962 recombination. *Genetics* 120:831-840.

963
 964 Hudson RR, Kaplan NL. 1995. Deleterious background selection with recombination. *Genetics*
 965 141:1605-1617.

966
 967 Huson DH, Klöpper T, Lockhart PJ, Steel MA. 2005. Reconstruction of Reticulate Networks from
 968 Gene Trees. In: Miyano S, Mesirov J, Kasif S, Istrail S, Pevzner PA, Waterman M, editors.
 969 *Research in Computational Molecular Biology. RECOMB 2005. Lecture Notes in Computer*
 970 *Science: Springer, Berlin, Heidelberg.*

971
 972 Jackman SD, Vandervalk BP, Mohamadi H, Chu J, Yeo S, Hammond SA, Jahesh G, Khan H,
 973 Coombe L, Warren RL, Birol I. 2017. ABySS 2.0: resource-efficient assembly of large genomes
 974 using a Bloom filter. *Genome Res* 27:768-777.

975
 976 Jarvis ED, Mirarab S, Aberer AJ, Li B, Houde P, Li C, Ho SY, Faircloth BC, Nabholz B, Howard
 977 JT, et al. 2014. Whole-genome analyses resolve early branches in the tree of life of modern birds.
 978 *Science* 346:1320-1331.

979
 980 Jensen-Seaman MI, Furey TS, Payseur BA, Lu Y, Roskin KM, Chen CF, Thomas MA, Haussler
 981 D, Jacob HJ. 2004. Comparative recombination rates in the rat, mouse, and human genomes.
 982 *Genome Res* 14:528-538.

983
984 Johri P, Aquadro CF, Beaumont M, Charlesworth B, Excoffier L, Eyre-Walker A, Keightley PD,
985 Lynch M, McVean G, Payseur BA, et al. 2022. Recommendations for improving statistical
986 inference in population genomics. *PLoS Biol* 20:e3001669.

987
988 Jones MR, Mills LS, Alves PC, Callahan CM, Alves JM, Lafferty DJR, Jiggins FM, Jensen JD,
989 Melo-Ferreira J, Good JM. 2018. Adaptive introgression underlies polymorphic seasonal
990 camouflage in snowshoe hares. *Science* 360:1355-1358.

991
992 Junier T, Zdobnov EM. 2010. The Newick utilities: high-throughput phylogenetic tree processing
993 in the UNIX shell. *Bioinformatics* 26:1669-1670.

994
995 Kalyaanamoorthy S, Minh BQ, Wong TKF, von Haeseler A, Jermiin LS. 2017. ModelFinder: fast
996 model selection for accurate phylogenetic estimates. *Nat Methods* 14:587-589.

997
998 Kaplan NL, Hudson RR, Langley CH. 1989. The "hitchhiking effect" revisited. *Genetics* 123:887-
999 899.

1000
1001 Kartje ME, Jing P, Payseur BA. 2020. Weak Correlation between Nucleotide Variation and
1002 Recombination Rate across the House Mouse Genome. *Genome Biol Evol* 12:293-299.

1003
1004 Katoh K, Standley DM. 2013. MAFFT multiple sequence alignment software version 7:
1005 improvements in performance and usability. *Mol Biol Evol* 30:772-780.

1006
1007 Katzman S, Kern AD, Bejerano G, Fewell G, Fulton L, Wilson RK, Salama SR, Haussler D. 2007.
1008 Human genome ultraconserved elements are ultraselected. *Science* 317:915.

1009
1010 Keane TM, Wong K, Adams DJ, Flint J, Reymond A, Yalcin B. 2014. Identification of structural
1011 variation in mouse genomes. *Front Genet* 5:192.

1012
1013 Kimura Y, Hawkins MT, McDonough MM, Jacobs LL, Flynn LJ. 2015. Corrected placement of
1014 *Mus-Rattus* fossil calibration forces precision in the molecular tree of rodents. *Sci Rep* 5:14444.

1015
1016 Kimura Y, Jacobs LL, Cerling TE, Uno KT, Ferguson KM, Flynn LJ, Patnaik R. 2013. Fossil mice
1017 and rats show isotopic evidence of niche partitioning and change in dental ecomorphology related
1018 to dietary shift in Late Miocene of Pakistan. *PLoS One* 8:e69308.

1019

1020 Kong A, Gudbjartsson DF, Sainz J, Jonsdottir GM, Gudjonsson SA, Richardsson B, Sigurdardottir
1021 S, Barnard J, Hallbeck B, Masson G, et al. 2002. A high-resolution recombination map of the
1022 human genome. *Nat Genet* 31:241-247.

1023
1024 Kowalczyk A, Meyer WK, Partha R, Mao W, Clark NL, Chikina M. 2019. RERconverge: an R
1025 package for associating evolutionary rates with convergent traits. *Bioinformatics* 35:4815-4817.

1026
1027 Kulathinal RJ, Stevison LS, Noor MA. 2009. The genomics of speciation in *Drosophila*: diversity,
1028 divergence, and introgression estimated using low-coverage genome sequencing. *PLoS Genet*
1029 5:e1000550.

1030
1031 Kumon T, Ma J, Akins RB, Stefanik D, Nordgren CE, Kim J, Levine MT, Lampson MA. 2021.
1032 Parallel pathways for recruiting effector proteins determine centromere drive and suppression. *Cell*
1033 184:4904-4918 e4911.

1034
1035 Calculating and interpreting gene- and site-concordance factors in phylogenomics [Internet]. The
1036 Lanfear Lab @ ANU2018 September 20, 2021]. Available from:
1037 http://www.robertlanfear.com/blog/files/concordance_factors.html

1038
1039 Lecompte E, Aplin K, Denys C, Catzefflis F, Chades M, Chevret P. 2008. Phylogeny and
1040 biogeography of African Murinae based on mitochondrial and nuclear gene sequences, with a new
1041 tribal classification of the subfamily. *BMC Evol Biol* 8:199.

1042
1043 Lewontin RC, Birch LC. 1966. Hybridization as a Source of Variation for Adaptation to New
1044 Environments. *Evolution* 20:315-336.

1045
1046 Li H. 2013. Aligning sequence reads, clone sequences and assembly contigs with BWA-MEM.
1047 arXiv preprint arXiv:1303.3997.

1048
1049 Li H. 2018. Minimap2: pairwise alignment for nucleotide sequences. *Bioinformatics* 34:3094-
1050 3100.

1051
1052 Liu X, Wei F, Li M, Jiang X, Feng Z, Hu J. 2004. Molecular phylogeny and taxonomy of wood
1053 mice (genus *Apodemus* Kaup, 1829) based on complete mtDNA cytochrome b sequences, with
1054 emphasis on Chinese species. *Mol Phylogenet Evol* 33:1-15.

1055
1056 Lopes F, Oliveira LR, Kessler A, Beux Y, Crespo E, Cardenas-Alayza S, Majluf P, Sepulveda M,
1057 Brownell RL, Franco-Trecu V, et al. 2021. Phylogenomic Discordance in the Eared Seals is best

1058 explained by Incomplete Lineage Sorting following Explosive Radiation in the Southern
1059 Hemisphere. *Syst Biol* 70:786-802.

1060

1061 Louca S, Pennell MW. 2020. Extant timetrees are consistent with a myriad of diversification
1062 histories. *Nature* 580:502-505.

1063

1064 Lundrigan BL, Jansa SA, Tucker PK. 2002. Phylogenetic relationships in the genus *mus*, based on
1065 paternally, maternally, and biparentally inherited characters. *Syst Biol* 51:410-431.

1066

1067 Maddison WP. 1997. Gene Trees in Species Trees. *Systematic Biology* 46:523-536.

1068

1069 Martin Y, Gerlach G, Schlotterer C, Meyer A. 2000. Molecular phylogeny of European muroid
1070 rodents based on complete cytochrome b sequences. *Mol Phylogenet Evol* 16:37-47.

1071

1072 Maynard Smith J, Haigh J. 1974. The hitch-hiking effect of a favourable gene. *Genet Res* 23:23-
1073 35.

1074

1075 McKenzie PF, Eaton DAR. 2020. The Multispecies Coalescent in Space and Time.
1076 [bioRxiv:2020.2008.2002.233395](https://doi.org/10.1101/2020.2008.2002.233395).

1077

1078 Mendes FK, Fuentes-Gonzalez JA, Schraiber JG, Hahn MW. 2018. A multispecies coalescent
1079 model for quantitative traits. *Elife* 7:e36482.

1080

1081 Mendes FK, Hahn MW. 2016. Gene Tree Discordance Causes Apparent Substitution Rate
1082 Variation. *Syst Biol* 65:711-721.

1083

1084 Mendes FK, Hahn Y, Hahn MW. 2016. Gene Tree Discordance Can Generate Patterns of
1085 Diminishing Convergence over Time. *Mol Biol Evol* 33:3299-3307.

1086

1087 Mendes FK, Livera AP, Hahn MW. 2019. The perils of intralocus recombination for inferences of
1088 molecular convergence. *Philos Trans R Soc Lond B Biol Sci* 374:20180244.

1089

1090 Mikula O, Nicolas V, Šumbera R, Konečný A, Denys C, Verheyen E, Bryjová A, Lemmon AR,
1091 Lemmon EM, Bryja J. 2021. Nuclear phylogenomics, but not mitogenomics, resolves the most
1092 successful Late Miocene radiation of African mammals (Rodentia: Muridae: Arvicanthini).
1093 *Molecular Phylogenetics and Evolution* 157:107069.

1094

1095 Minh BQ, Hahn MW, Lanfear R. 2020a. New Methods to Calculate Concordance Factors for
 1096 Phylogenomic Datasets. *Mol Biol Evol* 37:2727-2733.

1097

1098 Minh BQ, Schmidt HA, Chernomor O, Schrempf D, Woodhams MD, von Haeseler A, Lanfear R.
 1099 2020b. IQ-TREE 2: New Models and Efficient Methods for Phylogenetic Inference in the
 1100 Genomic Era. *Mol Biol Evol* 37:1530-1534.

1101

1102 Mirarab S, Nakhleh L, Warnow T. 2021. Multispecies coalescent: theory and applications in
 1103 phylogenetics. *Annual Review of Ecology, Evolution, and Systematics* 52:247-268.

1104

1105 Mölder F, Jablonski KP, Letcher B, Hall MB, Tomkins-Tinch CH, Sochat V, Forster J, Lee S,
 1106 Twardziok SO, Kanitz A, et al. 2021. Sustainable data analysis with Snakemake. *F1000Res* 10:33.

1107

1108 Moore EC, Thomas GWC, Mortimer S, Kopania EEK, Hunnicutt KE, Clare-Salzler ZJ, Larson
 1109 EL, Good JM. 2022. The Evolution of Widespread Recombination Suppression on the Dwarf
 1110 Hamster (Phodopus) X Chromosome. *Genome Biol Evol* 14:evac080.

1111

1112 Mouse Genome Sequencing C, Waterston RH, Lindblad-Toh K, Birney E, Rogers J, Abril JF,
 1113 Agarwal P, Agarwala R, Ainscough R, Alexandersson M, et al. 2002. Initial sequencing and
 1114 comparative analysis of the mouse genome. *Nature* 420:520-562.

1115

1116 Murrell B, Weaver S, Smith MD, Wertheim JO, Murrell S, Aylward A, Eren K, Pollner T, Martin
 1117 DP, Smith DM, et al. 2015. Gene-wide identification of episodic selection. *Mol Biol Evol* 32:1365-
 1118 1371.

1119

1120 Nilsson P, Solbakken MH, Schmid BV, Orr RJS, Lv R, Cui Y, Song Y, Zhang Y, Baalsrud HT,
 1121 Torresen OK, et al. 2020. The Genome of the Great Gerbil Reveals Species-Specific Duplication
 1122 of an MHCII Gene. *Genome Biol Evol* 12:3832-3849.

1123

1124 Oliver JC. 2013. Microevolutionary processes generate phylogenomic discordance at ancient
 1125 divergences. *Evolution* 67:1823-1830.

1126

1127 Pagès M, Fabre P-H, Chaval Y, Mortelliti A, Nicolas V, Wells K, Michaux JR, Lazzari V. 2016.
 1128 Molecular phylogeny of South-East Asian arboreal murine rodents. *Zoologica Scripta* 45:349-364.

1129

1130 Pamilo P, Nei M. 1988. Relationships between gene trees and species trees. *Mol Biol Evol* 5:568-
 1131 583.

1132

1133 Paradis E, Schliep K. 2019. ape 5.0: an environment for modern phylogenetics and evolutionary
1134 analyses in R. *Bioinformatics* 35:526-528.

1135

1136 Partha R, Kowalczyk A, Clark NL, Chikina M. 2019. Robust Method for Detecting Convergent
1137 Shifts in Evolutionary Rates. *Mol Biol Evol* 36:1817-1830.

1138

1139 Pease JB, Haak DC, Hahn MW, Moyle LC. 2016. Phylogenomics Reveals Three Sources of
1140 Adaptive Variation during a Rapid Radiation. *PLoS Biol* 14:e1002379.

1141

1142 Pease JB, Hahn MW. 2013. More accurate phylogenies inferred from low-recombination regions
1143 in the presence of incomplete lineage sorting. *Evolution* 67:2376-2384.

1144

1145 Platt RN, 2nd, Vandeweghe MW, Ray DA. 2018. Mammalian transposable elements and their
1146 impacts on genome evolution. *Chromosome Res* 26:25-43.

1147

1148 Pollard KS, Hubisz MJ, Rosenbloom KR, Siepel A. 2010. Detection of nonneutral substitution
1149 rates on mammalian phylogenies. *Genome Res* 20:110-121.

1150

1151 Pond SL, Frost SD, Muse SV. 2005. HyPhy: hypothesis testing using phylogenies. *Bioinformatics*
1152 21:676-679.

1153

1154 Poplin R, Ruano-Rubio V, DePristo MA, Fennell TJ, Carneiro MO, Auwera GAVd, Kling DE,
1155 Gauthier LD, Levy-Moonshine A, Roazen D, et al. 2018. Scaling accurate genetic variant
1156 discovery to tens of thousands of samples. *bioRxiv*:201178.

1157

1158 Ptak SE, Hinds DA, Koehler K, Nickel B, Patil N, Ballinger DG, Przeworski M, Frazer KA, Paabo
1159 S. 2005. Fine-scale recombination patterns differ between chimpanzees and humans. *Nat Genet*
1160 37:429-434.

1161

1162 Quinlan AR, Hall IM. 2010. BEDTools: a flexible suite of utilities for comparing genomic
1163 features. *Bioinformatics* 26:841-842.

1164

1165 R Core Team. 2021. R: A language and environment for statistical computing. Vienna, Austria.

1166

1167 Ranwez V, Douzery EJP, Cambon C, Chantret N, Delsuc F. 2018. MACSE v2: Toolkit for the
1168 Alignment of Coding Sequences Accounting for Frameshifts and Stop Codons. *Mol Biol Evol*
1169 35:2582-2584.

1170

1171 Revell LJ. 2012. phytools: an R package for phylogenetic comparative biology (and other things).
 1172 Methods in Ecology and Evolution 3:217-223.

1173

1174 Rivas-Gonzalez I, Rousselle M, Li F, Zhou L, Dutheil JY, Munch K, Shao Y, Wu D, Schierup
 1175 MH, Zhang G. 2023. Pervasive incomplete lineage sorting illuminates speciation and selection in
 1176 primates. Science 380:eabn4409.

1177

1178 Robinson DF, Foulds LR. 1981. Comparison of phylogenetic trees. Mathematical Biosciences
 1179 53:131-147.

1180

1181 Robinson DF, Foulds LR editors.; 1979 Berlin, Heidelberg.

1182

1183 Romanenko SA, Perelman PL, Trifonov VA, Graphodatsky AS. 2012. Chromosomal evolution in
 1184 Rodentia. Heredity (Edinb) 108:4-16.

1185

1186 Rosenberg NA. 2002. The probability of topological concordance of gene trees and species trees.
 1187 Theor Popul Biol 61:225-247.

1188

1189 Rowe KC, Achmadi AS, Fabre P-H, Schenk JJ, Steppan SJ, Esselstyn JA. 2019. Oceanic islands
 1190 of Wallacea as a source for dispersal and diversification of murine rodents. Journal of
 1191 Biogeography 46:2752-2768.

1192

1193 Roycroft E, Achmadi A, Callahan CM, Esselstyn JA, Good JM, Moussalli A, Rowe KC. 2021.
 1194 Molecular Evolution of Ecological Specialisation: Genomic Insights from the Diversification of
 1195 Murine Rodents. Genome Biol Evol 13:evab103.

1196

1197 Roycroft EJ, Moussalli A, Rowe KC. 2020. Phylogenomics Uncovers Confidence and Conflict in
 1198 the Rapid Radiation of Australo-Papuan Rodents. Syst Biol 69:431-444.

1199

1200 Sarver BA, Keeble S, Cosart T, Tucker PK, Dean MD, Good JM. 2017. Phylogenomic Insights
 1201 into Mouse Evolution Using a Pseudoreference Approach. Genome Biol Evol 9:726-739.

1202

1203 Scally A, Dutheil JY, Hillier LW, Jordan GE, Goodhead I, Herrero J, Hobolth A, Lappalainen T,
 1204 Mailund T, Marques-Bonet T, et al. 2012. Insights into hominid evolution from the gorilla genome
 1205 sequence. Nature 483:169-175.

1206

1207 Schenk JJ, Rowe KC, Steppan SJ. 2013. Ecological opportunity and incumbency in the
 1208 diversification of repeated continental colonizations by muroid rodents. Syst Biol 62:837-864.

1209
1210 Schliep KP. 2011. phangorn: phylogenetic analysis in R. *Bioinformatics* 27:592-593.

1211
1212 Serizawa K, Suzuki H, Tsuchiya K. 2000. A phylogenetic view on species radiation in *Apodemus*
1213 inferred from variation of nuclear and mitochondrial genes. *Biochem Genet* 38:27-40.

1214
1215 Shifman S, Bell JT, Copley RR, Taylor MS, Williams RW, Mott R, Flint J. 2006. A high-resolution
1216 single nucleotide polymorphism genetic map of the mouse genome. *PLoS Biol* 4:e395.

1217
1218 Singhal S, Leffler EM, Sannareddy K, Turner I, Venn O, Hooper DM, Strand AI, Li Q, Raney B,
1219 Balakrishnan CN, et al. 2015. Stable recombination hotspots in birds. *Science* 350:928-932.

1220
1221 Slatkin M, Pollack JL. 2006. The concordance of gene trees and species trees at two linked loci.
1222 *Genetics* 172:1979-1984.

1223
1224 Smagulova F, Gregoret IV, Brick K, Khil P, Camerini-Otero RD, Petukhova GV. 2011. Genome-
1225 wide analysis reveals novel molecular features of mouse recombination hotspots. *Nature* 472:375-
1226 378.

1227
1228 RepeatMasker Open-4.0 [Internet]. 2013-2015. Available from <http://www.repeatmasker.org>.

1229
1230 Smith BT, Merwin J, Provost KL, Thom G, Brumfield RT, Ferreira M, Mauck WM, Moyle RG,
1231 Wright TF, Joseph L. 2023. Phylogenomic Analysis of the Parrots of the World Distinguishes
1232 Artifactual from Biological Sources of Gene Tree Discordance. *Syst Biol* 72:228-241.

1233
1234 Smith MD, Wertheim JO, Weaver S, Murrell B, Scheffler K, Kosakovsky Pond SL. 2015a. Less
1235 is more: an adaptive branch-site random effects model for efficient detection of episodic
1236 diversifying selection. *Mol Biol Evol* 32:1342-1353.

1237
1238 Smith SA, Brown JW, Walker JF. 2018. So many genes, so little time: A practical approach to
1239 divergence-time estimation in the genomic era. *PLoS One* 13:e0197433.

1240
1241 Smith SA, Moore MJ, Brown JW, Yang Y. 2015b. Analysis of phylogenomic datasets reveals
1242 conflict, concordance, and gene duplications with examples from animals and plants. *BMC Evol*
1243 *Biol* 15:150.

1244
1245 Stanyon R, Yang F, Cavagna P, O'Brien P, Bagga M, Ferguson-Smith M, Wienberg J. 1999.
1246 Animal Cytogenetics and Comparative Mapping-Reciprocal chromosome painting shows that

1247 genomic rearrangement between rat and mouse proceeds ten times faster than between humans
1248 and cats. *Cytogenetics and Cell Genetics* 84:150-155.

1249
1250 Stapley J, Feulner PGD, Johnston SE, Santure AW, Smadja CM. 2017. Variation in recombination
1251 frequency and distribution across eukaryotes: patterns and processes. *Philos Trans R Soc Lond B*
1252 *Biol Sci* 372.

1253
1254 Steenwyk JL, Li Y, Zhou X, Shen XX, Rokas A. 2023. Incongruence in the phylogenomics era.
1255 *Nat Rev Genet* 24:834-850.

1256
1257 Steppan SJ, Adkins RM, Spinks PQ, Hale C. 2005. Multigene phylogeny of the Old World mice,
1258 Murinae, reveals distinct geographic lineages and the declining utility of mitochondrial genes
1259 compared to nuclear genes. *Mol Phylogenet Evol* 37:370-388.

1260
1261 Steppan SJ, Schenk JJ. 2017. Muroid rodent phylogenetics: 900-species tree reveals increasing
1262 diversification rates. *PLoS One* 12:e0183070.

1263
1264 Stevison LS, Woerner AE, Kidd JM, Kelley JL, Veeramah KR, McManus KF, Great Ape Genome
1265 P, Bustamante CD, Hammer MF, Wall JD. 2016. The Time Scale of Recombination Rate
1266 Evolution in Great Apes. *Mol Biol Evol* 33:928-945.

1267
1268 Sun C, Huang J, Wang Y, Zhao X, Su L, Thomas GWC, Zhao M, Zhang X, Jungreis I, Kellis M,
1269 et al. 2021. Genus-Wide Characterization of Bumblebee Genomes Provides Insights into Their
1270 Evolution and Variation in Ecological and Behavioral Traits. *Mol Biol Evol* 38:486-501.

1271
1272 Suzuki H, Shimada T, Terashima M, Tsuchiya K, Aplin K. 2004. Temporal, spatial, and ecological
1273 modes of evolution of Eurasian *Mus* based on mitochondrial and nuclear gene sequences. *Mol*
1274 *Phylogenet Evol* 33:626-646.

1275
1276 Tange O. 2018. GNU Parallel.

1277
1278 To TH, Jung M, Lycett S, Gascuel O. 2016. Fast Dating Using Least-Squares Criteria and
1279 Algorithms. *Syst Biol* 65:82-97.

1280
1281 Treaster S, Deelen J, Daane JM, Murabito J, Karasik D, Harris MP. 2023. Convergent genomics
1282 of longevity in rockfishes highlights the genetics of human life span variation. *Sci Adv*
1283 9:eadd2743.

1284

1285 van der Valk T, Pecnerova P, Diez-Del-Molino D, Bergstrom A, Oppenheimer J, Hartmann S,
 1286 Xenikoudakis G, Thomas JA, Dehasque M, Saglican E, et al. 2021. Million-year-old DNA sheds
 1287 light on the genomic history of mammoths. *Nature* 591:265-269.

1288
 1289 Vanderpool D, Minh BQ, Lanfear R, Hughes D, Murali S, Harris RA, Raveendran M, Muzny DM,
 1290 Hibbins MS, Williamson RJ, et al. 2020. Primate phylogenomics uncovers multiple rapid
 1291 radiations and ancient interspecific introgression. *PLoS Biol* 18:e3000954.

1292
 1293 Wang LG, Lam TT, Xu S, Dai Z, Zhou L, Feng T, Guo P, Dunn CW, Jones BR, Bradley T, et al.
 1294 2020. Treeio: An R Package for Phylogenetic Tree Input and Output with Richly Annotated and
 1295 Associated Data. *Mol Biol Evol* 37:599-603.

1296
 1297 White MA, Ane C, Dewey CN, Larget BR, Payseur BA. 2009. Fine-scale phylogenetic
 1298 discordance across the house mouse genome. *PLoS Genet* 5:e1000729.

1299
 1300 Yalcin B, Wong K, Agam A, Goodson M, Keane TM, Gan X, Nellaker C, Goodstadt L, Nicod J,
 1301 Bhomra A, et al. 2011. Sequence-based characterization of structural variation in the mouse
 1302 genome. *Nature* 477:326-329.

1303
 1304 Yang Z. 2007. PAML 4: phylogenetic analysis by maximum likelihood. *Mol Biol Evol* 24:1586-
 1305 1591.

1306
 1307 Yekutieli D, Benjamini Y. 1999. Resampling-based false discovery rate controlling multiple test
 1308 procedures for correlated test statistics. *Journal of Statistical Planning and Inference* 82:171-196.

1309
 1310 Yu G. 2020. Using ggtree to Visualize Data on Tree-Like Structures. *Curr Protoc Bioinformatics*
 1311 69:e96.

1312
 1313 Yu G, Smith DK, Zhu H, Guan Y, Lam TT-Y. 2017. ggtree: an r package for visualization and
 1314 annotation of phylogenetic trees with their covariates and other associated data. *Methods in*
 1315 *Ecology and Evolution* 8:28-36.

1316
 1317 Zhang C, Rabiee M, Sayyari E, Mirarab S. 2018. ASTRAL-III: polynomial time species tree
 1318 reconstruction from partially resolved gene trees. *BMC Bioinformatics* 19:153.

1319
 1320
 1321